6.3

Máster Universitario en Túneles y Obras Subterráneas

ÁREA: C6
MÓDULO: CONSTRUCCIÓN DE TÚNELES

SOLUCIONES CONTRA EXPANSIVIDAD Y COLAPSO

PONENTES: Pablo De la Fuente
Dr. I.C.C.P.
UPM

Día: 29/05/07
Hora: 16:00 A 18:00

ARTICLE IN PRESS

Available online at www.sciencedirect.com
SCIENCE DIRECT®

Tunnelling and Underground Space Technology xxx (2006) xxx–xxx

Tunnelling and Underground Space Technology
incorporating Trenchless Technology Research

www.elsevier.com/locate/tust

Design and optimisation of the lining of a tunnel in the presence of expansive clay levels

J. Pérez-Romero [a,*], C.S. Oteo [b], P. de la Fuente [c]

[a] University Alfonso X el Sabio, E.T.S. de Ingenieros de Caminos, Canales y Puertos, Avenida de la Universidad 1, Villanueva de la Cañada, 28691 Madrid, Spain
[b] University of A Coruña, E.T.S. de Ingenieros de Caminos, Canales y Puertos, Campus de Elviña, 15071 A Coruña, Spain
[c] Polytechnic University of Madrid, E.T.S. de Ingenieros de Caminos, Canales y Puertos, Ciudad Universitaria, 28040 Madrid, Spain

Abstract

This paper describes the study made of the Trasvasur tunnels (Canary Islands, Spain), which were excavated in rocky formations of volcanic origin presenting metric levels of expansive clays. The building of these tunnels had to be abandoned 30 years ago, owing to the problems caused by the expansivity of the ground. It was subsequently decided to resume the project, making joint use of geotechnical investigation campaigns, convergence measurements and numerical simulations, thereby contributing towards the optimisation of the cross-section of the tunnelled area, support and lining. The work done has shown that when building tunnels in the presence of expansive clays it is advisable to use circular or similar cross-sections. It has also been found to be advisable to seal off the excavation as quickly as possible to prevent alteration due to the decompression of the expansive clay levels and their absorbing water from the tunnel itself.
© 2006 Elsevier Ltd. All rights reserved

Keywords: Tunnel; Expansive clay; Numerical analysis; Convergence measurements

1. Introduction

The Trasvasur tunnels are part of a set of hydraulic Works connecting several dams in the south of the island of Gran Canaria (Canary Islands, Spain) to the Tirajana Gorge. The water-transfer channel has an average slope of 0.3% and a total length of 13.8 km, of which 10.2 km run through a tunnel to be excavated by ripper. The works commenced in 1974 but were interrupted shortly afterwards because of the instability problems found in the tunnels known as tunnel IV and tunnel V. In both cases the instability was associated with the presence of levels of expansive clay embedded in a rocky matrix with varying degrees of alteration. Fig. 1 schematically illustrates the state of the works when they were interrupted.

Tunnel IV had been designed to have a total length of 3148 m, of which 1206 m was built from mouth 3, located in the Fataga Gorge, and 434 m from mouth 4, located in the Vicentes Gorge. The sections built had been lined with concrete 0.20–0.30 m thick in the side-wall and crown areas, but the floors had not yet been lined when the work was stopped. In 1995 the state of the tunnel was inspected (Fig. 2) and the lining was found to be deformed and seriously cracked between kilometre points 0+715 and 0+840. Fig. 3 schematically illustrates the damage found, consisting of the breakage of the lining key, where the clay appears at the top of the tunnelled area, as well as major horizontal deformation of the lining where the clay levels are located in side-wall or floor areas.

Tunnel V is 2844 km long, of which 464 m had been excavated from mouth 1, located in the Tirajana Gorge, and 870 m from mouth 2, which like mouth 3 is located in the Fataga Gorge. Since much of the work done was tunnelled in healthy rock no lining had been placed. When this tunnel was inspected, the floor had risen considerable between kilometre points 0+670 and 0+880, as Fig. 4 shows, swing to the intrusion of terrain from a clay level

* Corresponding author. Fax: +34958279124/2231214.
E-mail address: joaquin.perez@auna.com (J. Pérez-Romero).

0886-7798/$ - see front matter © 2006 Elsevier Ltd. All rights reserved
doi:10.1016/j.tust.2006.02.002

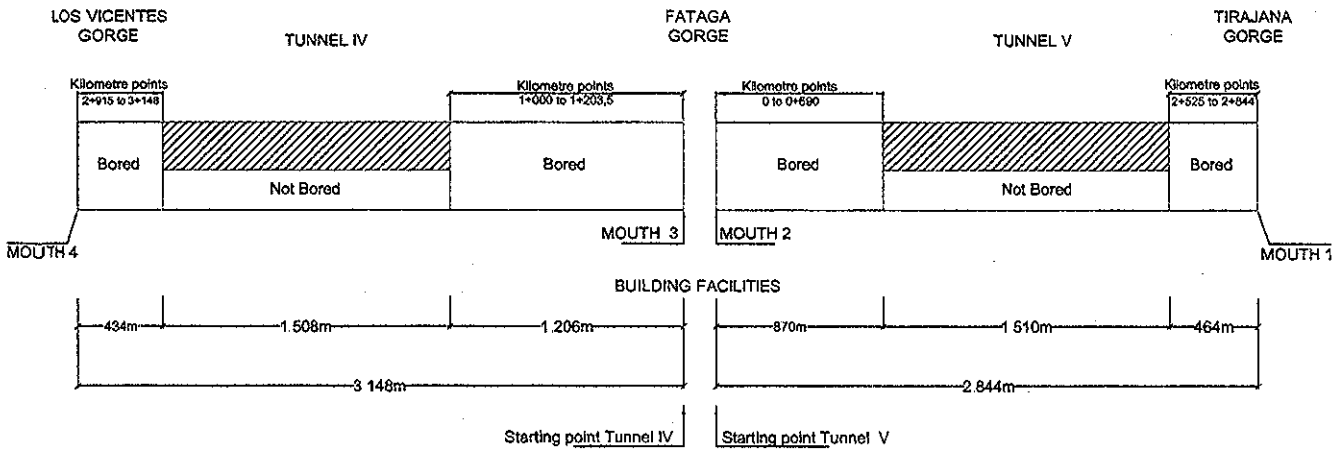

Fig. 1. State of the works when they were interrupted

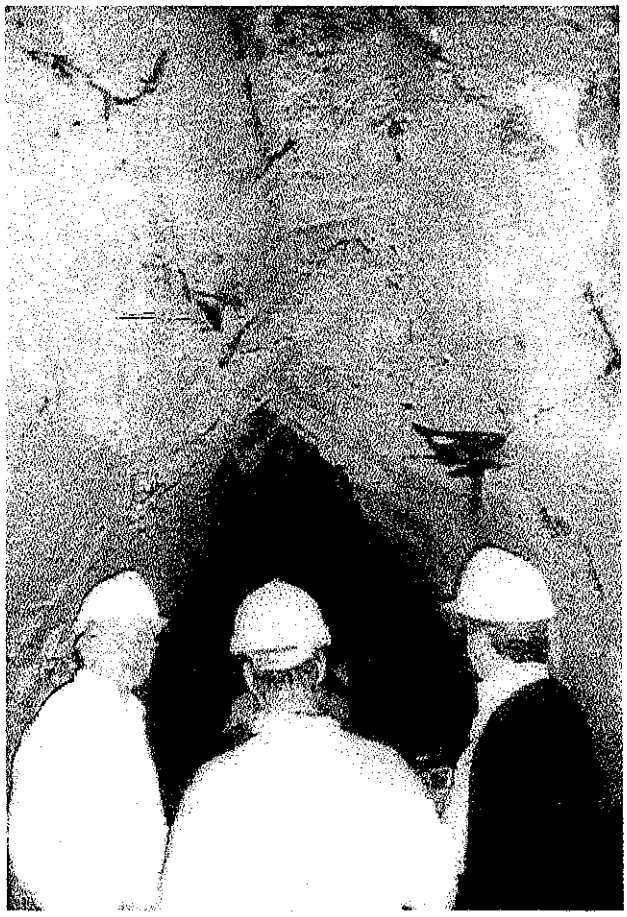

Fig. 2. State of tunnel IV in 1995

that was located in the lower part of the tunnelled section (Fig. 5).

The project was resumed about 25 years later, with a view to completing these tunnels. A total of six different sections were designed, to be supported by grout 0.05–0.20 m thick, bolts injected with resin and arcwelded mesh.

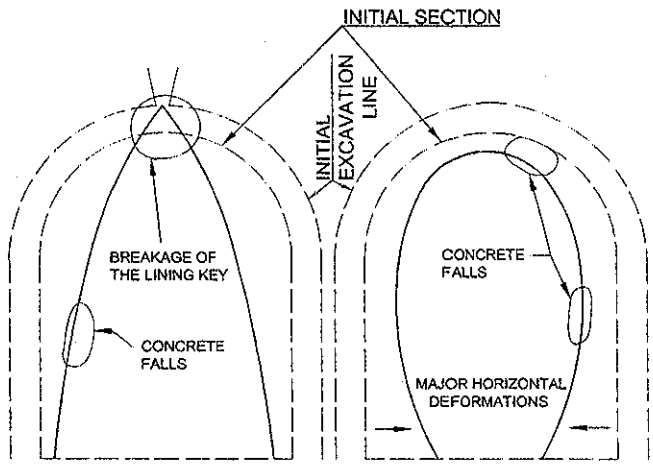

Fig. 3. Damage observed in tunnel IV

The interior housed a "U"-shaped reinforcedconcrete channel, as shown in Fig. 6.

2. Geological framing

Fig. 7 shows the geological profile of tunnels IV and V, indicating the sections tunnelled before the Works were abandoned in 1974.

The base level in the area consists of sub-horizontal layers of ignimbrites composed of pyroclastic fragments of sand and silt embedded in a clay matrix (Fig. 8c). In some levels the clay fraction is clearly dominant, and smectite concentrations of over 90% have been detected (mainly montmorillonite and Na-montmorillonite).

Above the ignimbrites phonolitic lava flows are found (Astudillo et al., 1994), consisting of latites and quartzlatites with the usual hypocrystalline, phaneritic, porphyritic and vesicular flow structure (Fig. 8b). Expansive clay levels of volcanic tuffs have been identified, of decimetric and even metric thickness, located between the phonolitic (Fig. 8a). Finally, in the more superficial areas colluvial

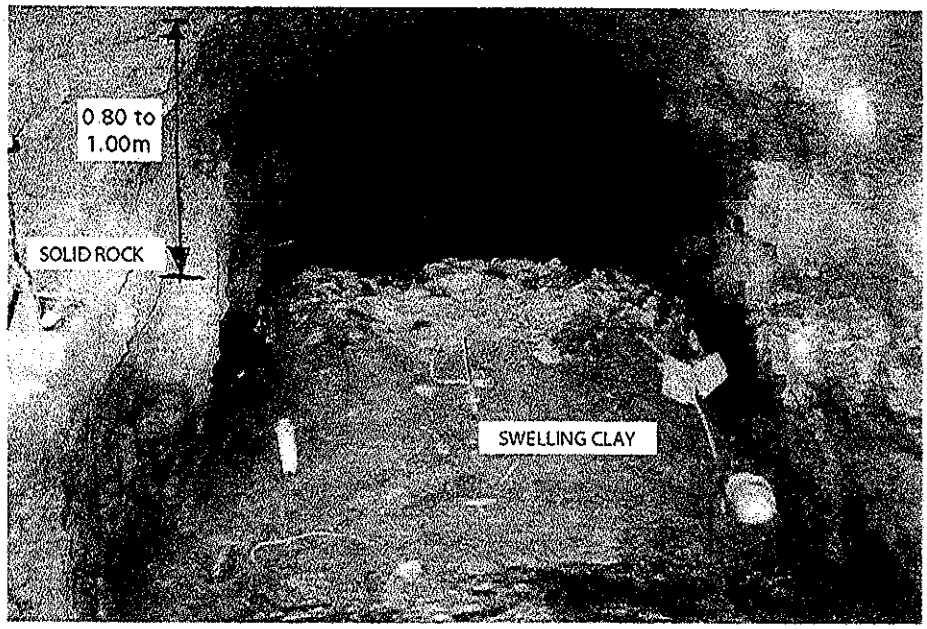

Fig 4. State of tunnel V in 1995

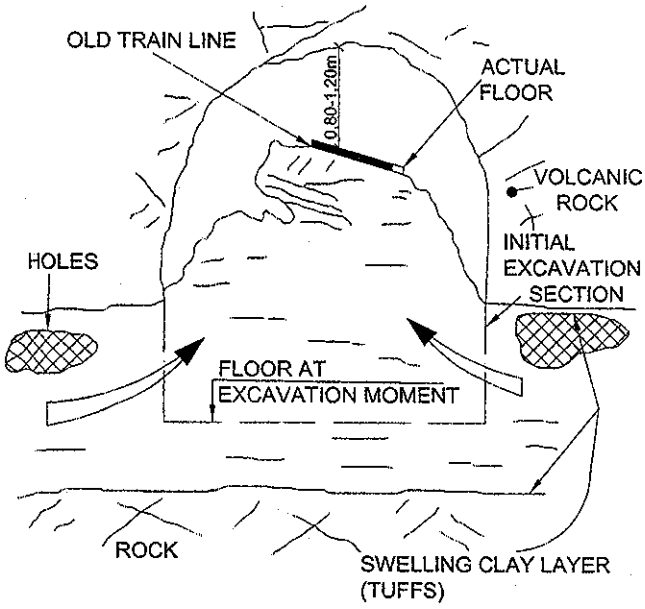

Fig 5 Damage observed in tunnel V

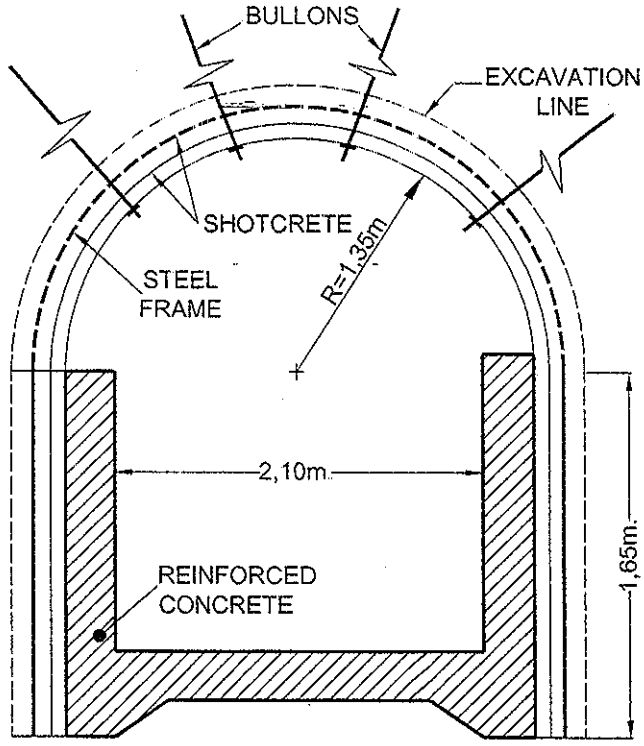

Fig 6 Project cross-section in unstable areas

and eluvial levels appear, resulting from the disturbance of the underlying formations.

The route of tunnels IV and V passes through all the materials mentioned above. Specifically, the route of tunnel V is located in a thick formation of ignimbrites containing a highly plastic and expansive clay level located both in the side-wall area and beneath the floor of the tunnel section, whereas tunnel IV mostly passes through phonolites with the presence of a significant subhorizontal level of volcanic tuffs, which are also expansive and highly plastic, up to 2.50 m thick, appearing above the tunnel crown and descending below the floor.

There is a clear link between the presence of these highly plastic expansive clay levels and the pathologies described above that forced the works to be abandoned

ARTICLE IN PRESS

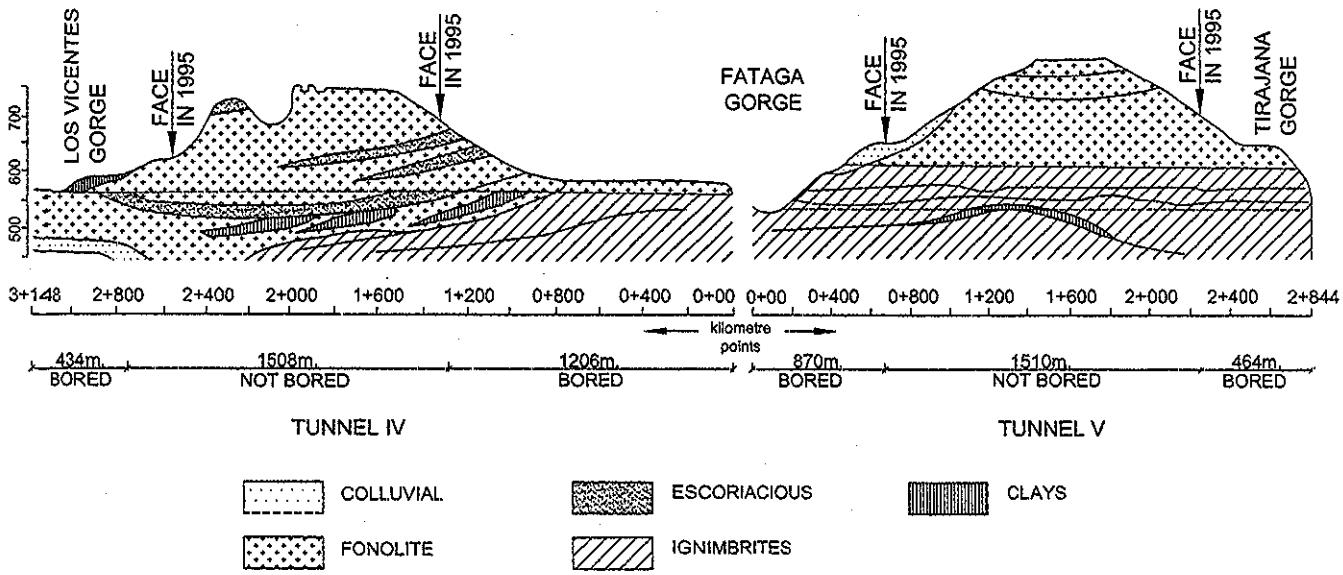

Fig 7 Geological profile of tunnels IV and V

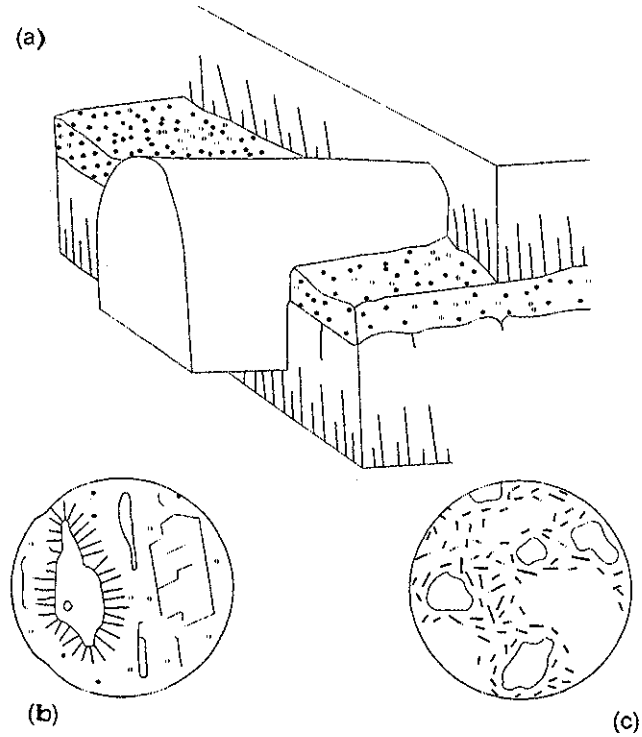

Fig 8 Texture of the lava flows and expansive pyroclastic levels

3. Geotechnical characterisation of the materials

In 1995 a new construction firm (Dragados) began to work on the completion of tunnels IV and V. A number of geotechnical research studies were commissioned from the consulting firm Intensa-Inarsa, in order to design solutions for the expansive clay areas.

In this section the prospecting work and laboratory tests that were carried out, mostly to characterise the compressibility properties, expansive potential and structure of the clay levels that had affected and damaged tunnels IV and V, are described. In areas presenting the most serious expansivity problems, six rotating boreholes with continuous core-sample recovery were drilled in the interior of tunnels IV and V. The clay levels were found to be 0.10–2.50 m thick.

Laboratory tests were performed on nine paraffin samples extracted form the boreholes, and on six samples obtained with a thin-wall sampler in superficial parts of the tunnelled areas. It should be clarified that by the time the sampling was done the tunnels had been abandoned for nearly 20 years after they were first excavated, and they had sometimes been used as water-storage tanks, so the properties of the ground close to the tunnelling perimeter were affected by the consequent decompression and moisture changes.

Table 1 shows the results of the laboratory tests carried out on these samples. As can be seen, the samples taken near to the tunnelling perimeter (samples MA-1 to MA-6) have a higher relative water content, generally presenting higher liquidity indices (LI), and a considerable lower dry density (γ_d); the degrees of saturation (Sr) of these samples are very high, sometimes approaching 100%. This demonstrates the intense alteration of the clay near the tunnelled areas, where it has undergone major tensional relaxation and an increase in moisture from the excavation itself.

A further indication of the alteration that the clay had undergone can be found in the values for resistance to unconfined compression in the interior of the boreholes ranged between 400 and 1200 kPa, whereas the decompressed clay close to the tunnelled area presented values of around 30 kPa.

With regard to the expansive potential of the clay, swelling-pressure values were zero to highly variable, between

Table 1
Index properties for samples from tunnels IV and V

Sample	Prospect	Tunnel	Kilometre point	Dry specific weight γ_d (kN/m^3)	Percentage of fines (%)	Water content in situ (%)	LL (%)	PL (%)	PI (%)	LI (%)	Sr (%)	USCS
MI-1	S2	IV	0+825	15.5	99	9	0	0	0	–	35	ML
MI-2	S4	IV	0+760	12.0	97	–	114	44	70	–	–	CH
MI-3	S4	IV	0+760	12.9	100	4	137	47	90	−0.5	8	CH
MI-4	S4	IV	0+760	13.2	99	34	129	56	73	−0.3	91	MH
MI-5	S4	IV	0+760	15.5	100	24	115	48	67	−0.4	92	MH
MI-6	S6	V	0+645	–	100	–	84	48	36	–	–	MH
MI-7	S6	V	0+645	–	100	–	86	45	41	–	–	MH
MI-8	S6	V	0+645	–	99	–	85	48	37	–	–	MH
MI-9	S5	V	0+675	19.6	92	–	54	23	31	–	–	CH
MA-1	–	IV	0+820	10.0	91	64	208	44	164	0.1	100	CH
MA-2	–	IV	0+814	10.2	90	60	198	49	149	0.1	100	CH
MA-3	–	IV	0+805	13.3	36	21	79	38	41	−0.4	57	MH
MA-4	–	V	0+685	13.6	64	27	78	29	49	0.0	77	CH
MA-5	–	V	0+698	10.5	94	51	103	45	58	0.1	90	MH
MA-6	–	V	0+705	15.8	30	25	79	28	51	−0.1	98	GC

180 and 1600 kPa, depending on the moisture content, while the values for free volumetric swelling during soaking exceeded 15%. In situations of semiconfinement, the volumetric-swelling values ranged between 4.5% and 12.5%, which gives some idea of the major expansive potential of the clay levels.

Six X-ray diffraction tests were performed, with very high smectite percentages being found, in general close to 90%, which are clearly related to the expansive nature of the formation.

Finally, five oedometric tests were carried out, the results of which allow the structure of the clay and the manner in which it is altered by the decompression and swelling processes to be studied (Pérez-Romero et al., 2002). In Fig. 9 the deformation curves are presented in a representation plane with the standardised voids index (Iv, Burland, 1990) compared with the effective vertical pressure (at logarithmic scale). The intrinsic compression line (ICL) and sedimentation compression line (SCL) proposed by Burland (1990) for clays have been indicated on this plane, as has the value for the effective vertical yield stress ($\sigma vy'$) for each test performed. Samples *B*, *C* and *D* were taken from the interior of the boreholes, while the remaining two samples (*F* and *H*) are disturbed, having been taken from the tunnelling perimeter. As it can be seen, the behaviour of the samples largely depends on the site where they were taken. Thus, the samples from the tunnelling perimeter present a higher value for the standardised voids index (Iv), while for vertical-stress range applied, the samples from the interior of the boreholes are highly overconsolidated and also present somewhat higher values for effective vertical yield stress.

In short, the evidence is clear that the conditions of deposition of these clays, possibly at high temperatures, have provided their structure with a fabric of particle bonds that play a decisive role in their mechanical behaviour.

Considering all the data available, geotechnical parameters have been assigned for the clay levels and for the solid rock (Table 2).

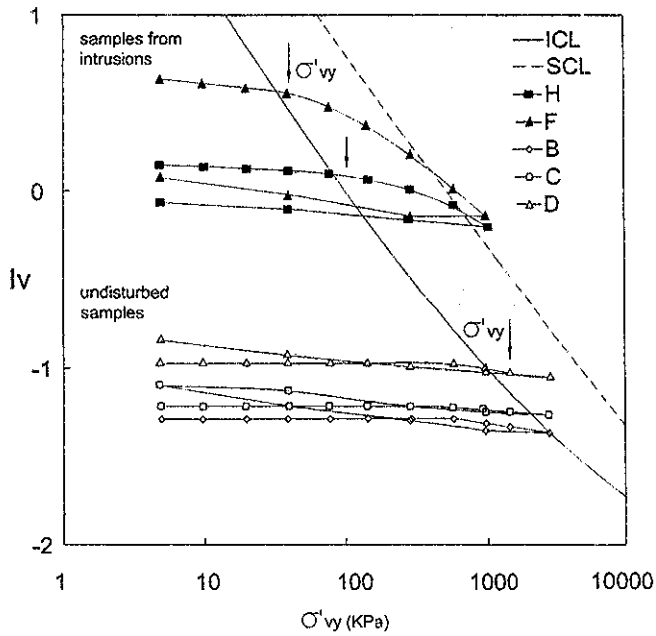

Fig. 9. Oedometric tests of expansive clay samples.

4. Results from the building of an experimental tunnel

Once the properties of the expansive clays had been determined, the possibility of altering the cross-section of the project was studied, as shown in Fig. 6, to which end a numerical analysis was performed on the interaction between the tunnel excavation and lining (Oteo et al., 1999). An elastic model of the terrain and two hypotheses for its expansivity were considered: the first with volumetric expansion of up to 2% throughout the tunnelling perimeter, and the other incorporating the presence of an expansive horizontal layer 1.50 m thick centred on the axis of the tunnel. The laws of bending moments and maximum stresses forecast were compared for three different cross-sections: the project crosssection (horseshoe/with a semi-

Table 2
Geotechnical parameters of the expansive clay levels and solid rock

Material	Symbol	Parameter	Units	Value
Expansive clay	G_s	Specific weight of solid particles	kN/m^3	26 7
	K	Permeability coefficient	m/s	$1 \times 10^{-8}\ S_r^3$
	ϕ'	Angle of shearing resistance	°	22^0
	K_0	Coefficient of earth pressure at rest	–	0.8
	LL	Liquid limit	%	80
	e_L	Void ratio at liquid limit	–	2 18
	C_c^*	Intrinsic compression index	–	0 5181
	C_c	Compression index	–	0 4 C_c^*
	C_s	Swelling index	–	0 1 C_c^*
Solid rock	γ	Unit weight of rock	kN/m^3	20
	E	Young's modulus	MPa	1500
	ν	Poisson's coefficient	–	0.2
	ucs	Unconfined compression strength	MPa	50

circular arch), a circular cross-section and an oval cross-section (Fig 10) The numerical analysis revealed that the project cross-section was not ideal, since it had to bear the highest bending moments, while the optimal possible behaviour was offered by the circular cross-section

It was not considered advisable to use the tunnel sections that had been previously damaged, since working inside them would be too dangerous The building of a bypass was proposed to avoid the affected sections, the axis of would lie at a distance of 15 m This change in the horizontal route would not create any problems because the purpose of the tunnels was to house a water channel

It was decided to build an experimental tunnel that would provide enough information to allow the remainder of the Project to be undertaken with the necessary safeguards Fig 11 shows the cross-section considered ("SC") for the sections suffering from the presence of expansive clays This cross-section has a circular inner perimeter, supported by steel frames, Bernold sheets and a layer of sprayed concrete 0 07 m thick The support base would be made of concrete that was reinforced immediately, in

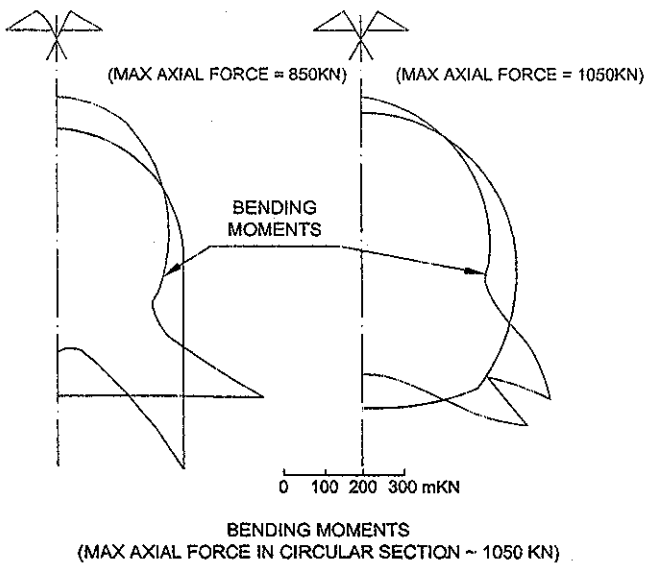

Fig 10 Stress laws for two sections and volumetric expansion for the entire perimeter of the tunnelled area

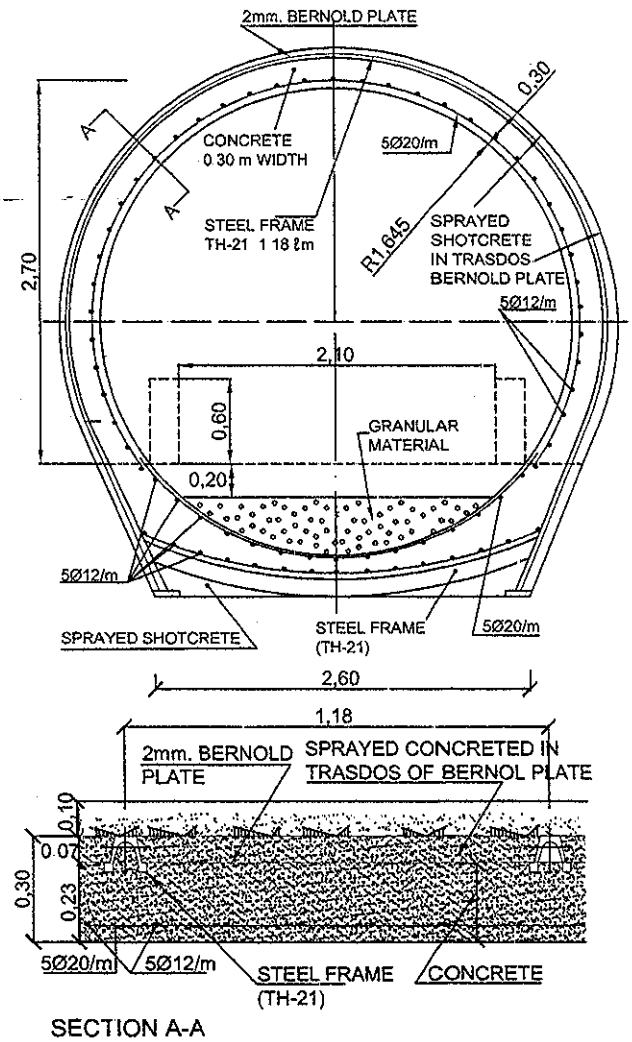

Fig 11 Cross-section (SC) considered for the experimental tunnel in expansive clay areas

order to increase its horizontal rigidity. Finally, a concrete lining would be fitted, working backwards, to obtain a section with a total thickness of un 0.30 m. For part of the route (SC') it was decided not to place the final concrete lining, in order to enable the influence of the lining on the behaviour of the tunnelling area to be studied.

Fig. 12 shows an alternative, less reinforced cross-section, which would be used for the first sections of the experimental tunnel to compare its behaviour with that of the previous ones (sections SC and SC'). At the beginning of the experimental galleria two different cross-sections were used: cross-section IV, with a sprayed-concrete lining, and cross-section V, which was further

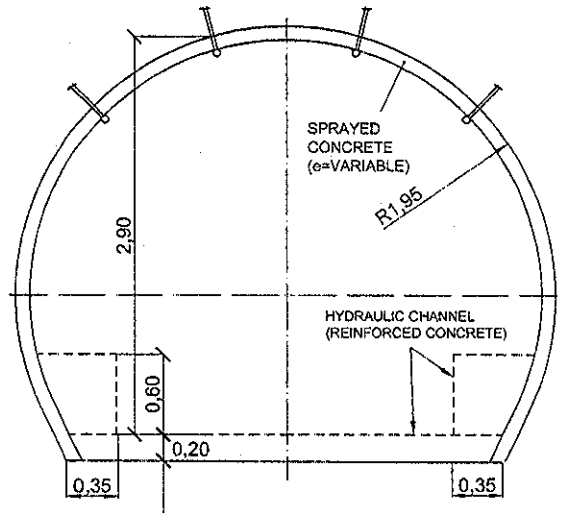

Fig. 12. Alternative cross-section (IV and V) considered for the experimental tunnel.

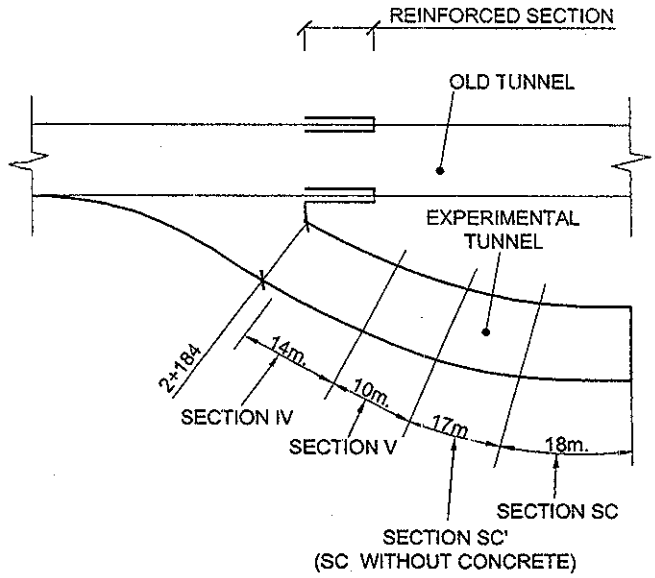

Fig. 13. Plan of the experimental gallery executed in tunnel V.

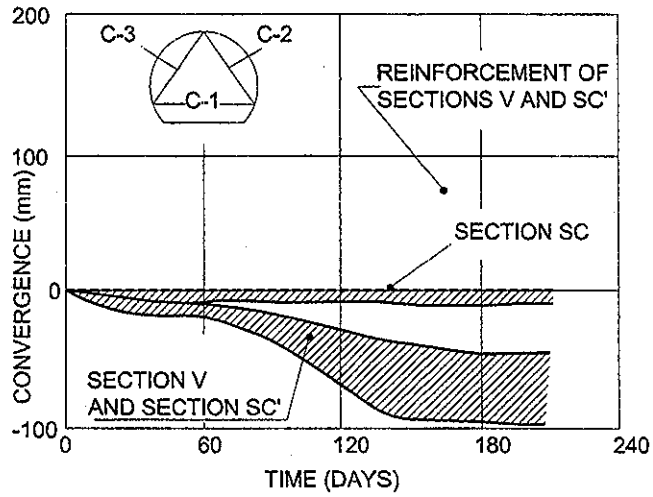

Fig. 14. Convergences measured in the experimental gallery.

reinforced with steel frames and Bernold sheets. Fig. 13 shows a plan of the experimental gallery, indicating the cross-sections used for each tunnel section (two new SC and SC' cross-sections and two that were the same as those in project IV and V).

Convergence measurements were taken in the experimental gallery, the results of which are presented in Fig. 14. The behaviour of the complete section (SC) was satisfactory, since any deformation was stabilised as soon as the floor was reinforced, and the convergence values recorded were lower than 0.01 m. However, in the other sections (IV, V and SC') deformation that increased over time was recorded, reaching 0.08 m, which meant that the base had to be reinforced as the final stabilisation measure.

5. Numerical and parametric analysis of the interaction between the tunnel excavation and the support

5.1. Description of the numerical analysis

The building of the experimental galleries demonstrated the feasibility of the solution and highlighted the difference between the behaviour of sections that had been reinforced to greater or lesser degrees. For these reasons a parametric study was carried out, based on numerical analysis, to determine the relative influence between the various different factors present in the project (Pérez-Romero, 2000). The following variables were taken into account:

A. Excavation cross-section: semicircular (Fig. 15a), circular (Fig. 15b) and round arch (horseshoe – Fig. 15c).
B. Position of the expansive clay level: crown, side walls and floor.
C. Thickness of the expansive clay level: 1 and 2 m thick.
D. Free volumetric swelling of the clay: 0% (nonexpansive), 2.5% and 5.0%.

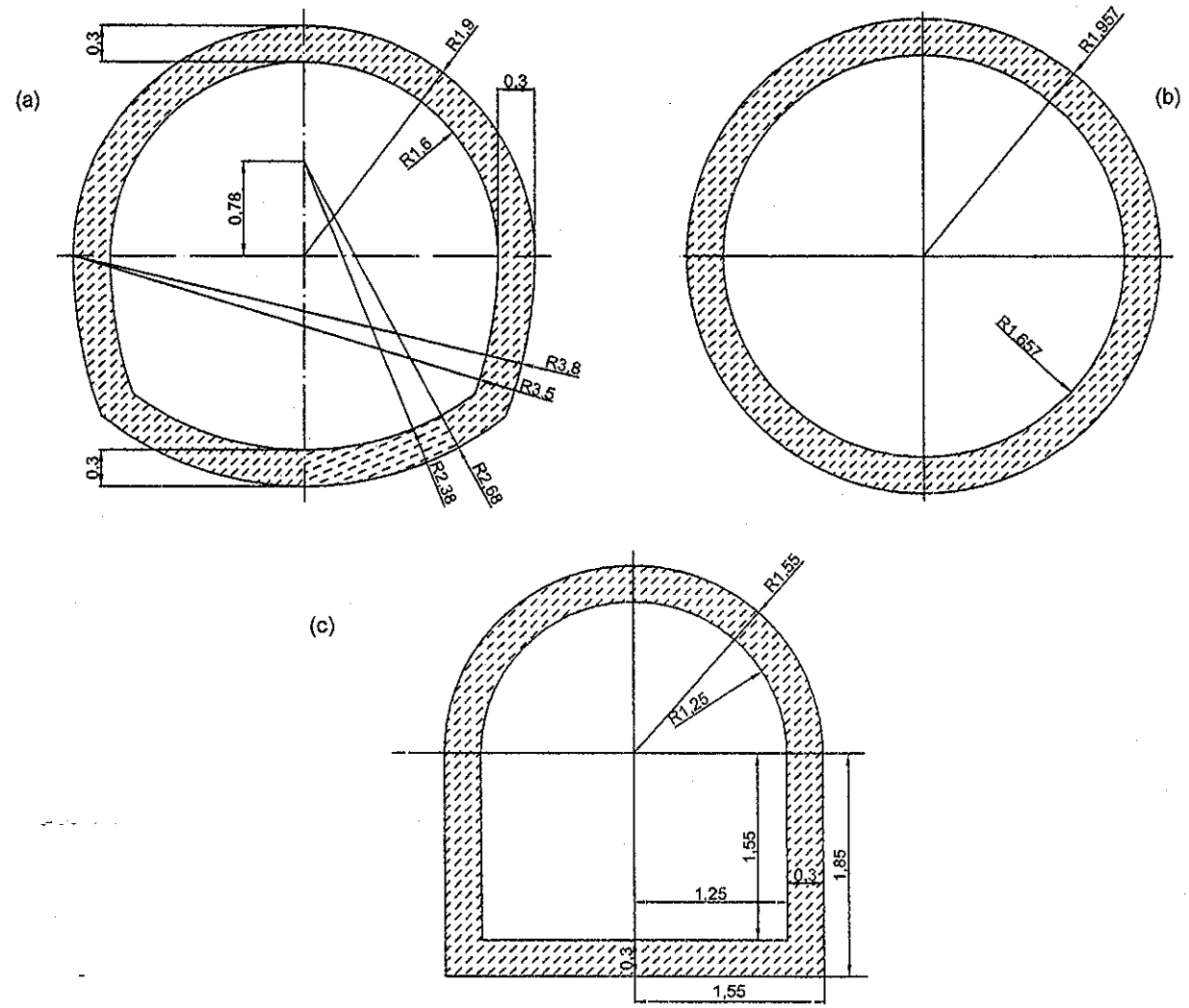

Fig. 15. Excavation and lining cross-sections considered in the parametric analysis.

E. Depth of the tunnel axis: 18, 30 and 50 m.
F. Lining: concrete perimeter lining 0.30 m thick (similar to section SC in the experimental gallery), concrete lining 0.30 m thick on the crown and side walls but not in the floor area (similar to section SC′ in the experimental gallery), and finally concrete lining 0.30 m thick on the floor and sprayed-concrete lining 0.05 m thick on the side walls and crown (similar to Section 5 of the experimental gallery).

These variables were combined to generate a total of 28 different scenarios, named according to the nomenclature given in Table 3.

Fig. 16 shows the finite-element mesh used for the calculations.

The constitutive model used for the calculation was that of a partially saturated soil. The clay levels were described by a critical-state model (modified Cam-clay) and the solid rock was simulated by means of an elastic model. For both materials the parameters deduced from the laboratory tests shown in Table 2 were used. Once a geostatic stress state in equilibrium had been obtained, the elements corresponding to the excavation cross-section were eliminated, such that the normal pressure at the limit of the excavation was cancelled. A boundary condition was later imposed for zero suction on the perimeter of the excavation, starting a process of saturation on the ground that progressed inwards. A certain time after the excavation the lining was placed, at which time an impermeable perimeter of the tunnelled area was obtained.

5.2. Behaviour of the tunnelled area

It is interesting to note the tenso-deformational behaviour of the ground near the tunnelled area. A good case in point is the one called "cs28t", consisting of a circular excavation with an expansive level (tuffs) 2 m thick located at the level of the axis (Fig. 17). The lining corresponds to a thickness of 0.30 m of concrete for the entire perimeter of the tunnelled area (Fig. 15b).

Table 3
Nomenclature of cases studied in parametric analysis

1st Letter	Tunnel section	o	ovoidal
		c	circular
		h	horseshoe – round arch
2nd Letter	Position of the swelling layer	v	vertex (crown)
		s	sidewall
		f	floor
3rd Letter	Thickness and change in volume of the swelling layer	1	1 m thick – 2.5% volume increase upon soaking
		2	2 m – 2.5%
		n	2 m – 0%
		d	2 m – 5%
4th Letter	Depth of the tunnel axis	8	18 m
		3	30 m
		5	50 m
5th Letter	Lining	t	concrete perimeter lining 0.30 m thick (similar to section SC in the experimental gallery)
		p	concrete lining 0.30 m thick on the crown and side walls but not in the floor area (similar to section SC′)
		g	concrete lining 0.30 m thick on the floor and sprayed-concrete lining 0.05 m thick on the side walls and crown (similar to section V)

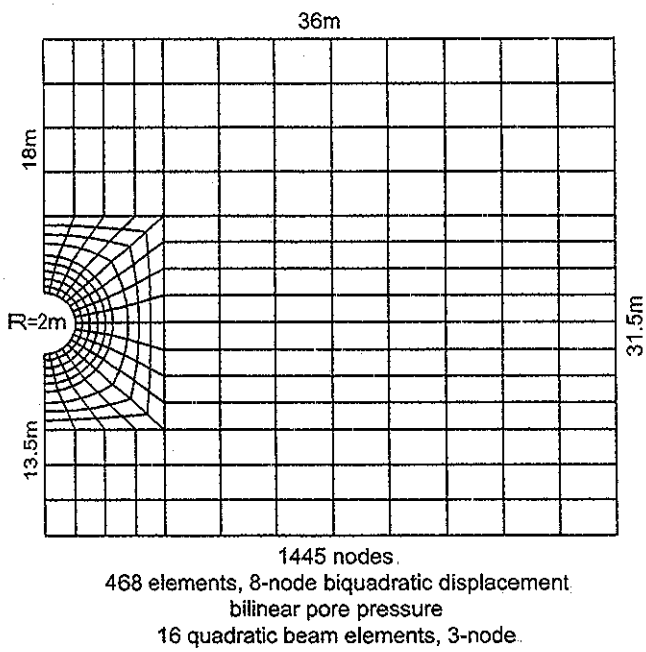

Fig. 16. Finite-element mesh used in the parametric analysis

Fig. 18 shows the changes in the voids ratio (e) and the angular deformation ($\delta\varepsilon$) one hour, one day and one week after the excavation. The combined effect of the decompression of the material, the swelling because of expansivity and the proximity of the clay to a critical state generates

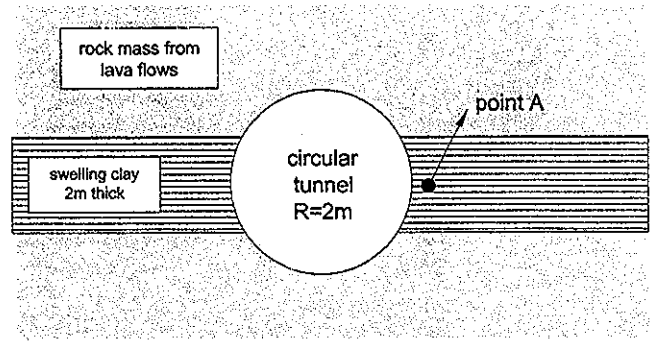

Fig. 17. Diagram of a case study (cs28t)

volume increases of up to 4.5% and angular deformations of over 3%.

Fig. 19 shows the stress–strain path of a point located in the expansive clay level (point A in Fig. 17). The initial site conditions have been marked with a white dot. Owing to the excavation of the tunnel, point A describes an stress decompression path (using the Cambridge variables: p' mean pressure, q deviatoric stress) that approaches the critical-state line (Fig. 19a), which explains the angular deformations estimated in the calculation and the creeping processes observed in 1995 in the unsupported sections (Figs. 4 and 5).

The volumetric change estimated (Fig. 19b) has two parts: an initial section where the volume increases, associated with the decompression of the clay, and another section where the volume also increases but as a result solely of its expansive potential. The first section is the result of the mechanical interaction between the excavation, the support and the lining, such that fewer deformations will occur in sections where the support is closed and thicker. The second section mentioned is related to the supply of moisture from inside the tunnelled area (which houses a water channel) and the expansive potential of the clay. These factors are favoured if the perimeter of the tunnelled area is not sealed off.

Finally, the influence of the clay structure on its mechanical behaviour has been described above, with diagenetic bonds between particles. The undisturbed samples were found to have a lower expansive potential than the samples taken from where the ground intrudes into the tunnelled area, which are extremely disturbed and partially remoulded, affecting their diagenetic bonds. Thus, the decompression and swelling phenomena have a positive synergy effect, since the alteration of the clay implies greater expansive potential, which in turn leads to greater deformation of the clay structure, with the consequent destruction of bonds between particles.

5.3. *Parametric analysis of results*

Table 4 shows the results of the 28 cases analysed: maximum stresses in the lining and estimated displacements on the crown, side walls and floor.

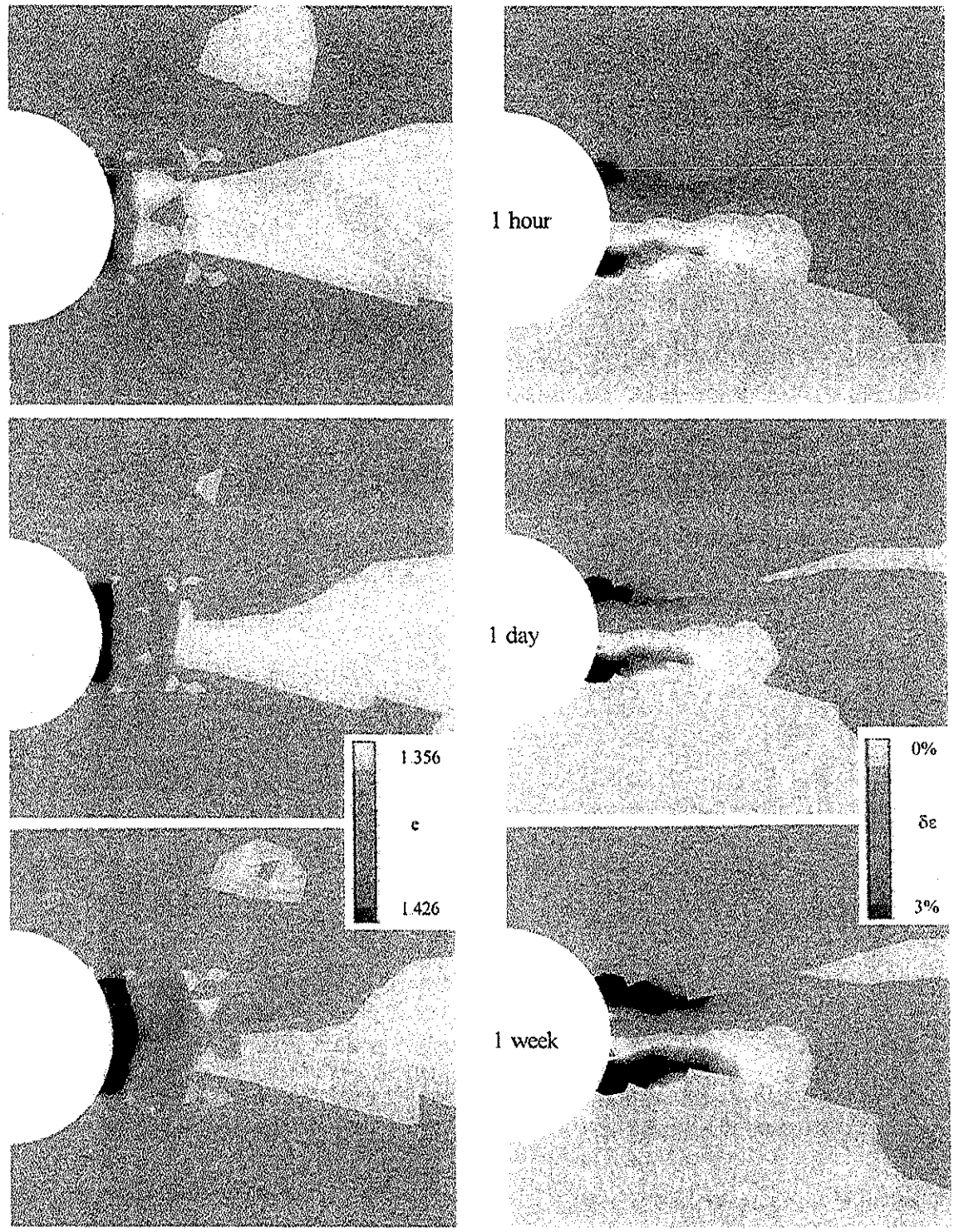

Fig. 18. Deformations estimated in the proximity of the tunnelled area

It is found that the most damaging position for a clay level harmful is on the side walls, at the same height as the axis of the tunnel, since this is where the highest stresses in the lining are generated. Fig. 20 shows the bending moments estimated for the three sections of the tunnelled area. It is clear that the excavation planned in the building project (Fig. 6) is the one that works the worst, while the section tested in the experimental gallery seems to be optimal (Fig. 11), being subjected to the smallest bending moments.

According to the results of the numerical analysis, the linings with grout 0.05 m thick are subjected to very high

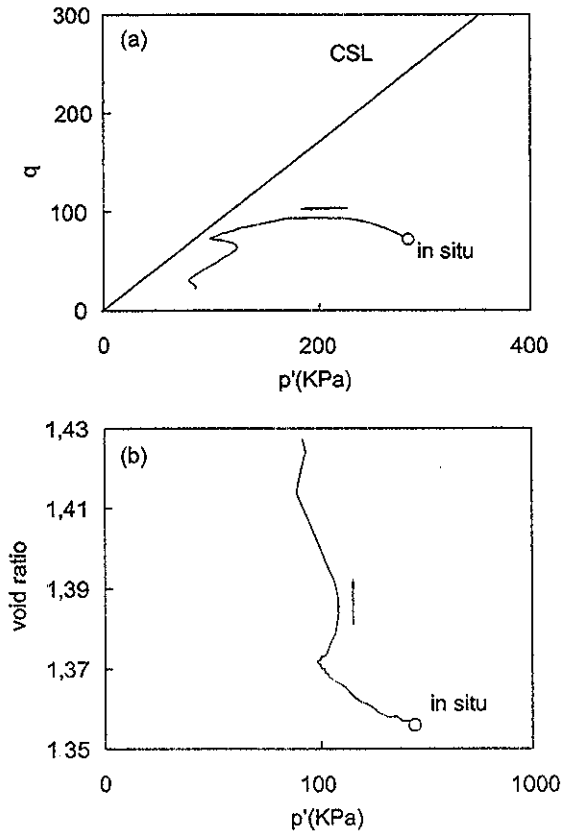

Fig 19—Stress–strain path of a point close to the tunnelled area

stresses, which is consistent with the behaviour observed in section SC′ of the experimental gallery, which had to be reinforced with 0 30 m of concrete lining. It is advisable for the lining to be applied to the entire perimeter of the tunnelled area in order to make the section watertight and prevent the clay from continuing to absorb water. Finally, the results of the numerical analysis of sections with concrete linings 0 30 m thick enables convergences of 0.01–0 03 m to be estimated, i.e. similar values to those for the convergences measured in the experimental tunnel.

Table 5 summarises the relative importance of the factors considered, among which the position of the expansive layer and its swelling potential, the cross-section of the tunnelled area and the support and lining thickness particularly stand out.

6. Optimisation of the lining during the course of the works

Once the studies reported above had been carried out, the works commenced, using the cross-section design shown in Fig. 11, with the following construction phases.

Phase 1:

1 1. Excavation in 1 40 m advance sections
1 2. Fitting TH-21 trusses.
1 3. Fitting Bernold sheets welded to the truss wings.

Table 4
Summary of results for a series of different cases

CASE	Maximum stresses in the lining		Estimated displacements		
	Tensile (MPa)	Compression (MPa)	Downwards at crown (mm)	Inwards at side walls (mm)	Upwards at floor (mm)
hv28t	0 38	−0 56	−23 4	−4 0	2 0
hs28t	12 33	−10 97	−6 2	−22 7	2 3
hf28t	2 68	−3 70	−1 4	−2 6	18 7
cvn8t	0 55	−0 81	−17 0	−2 5	2 0
cv28t	0 79	−2 14	−18 4	−2 3	1 5
cvd8t	1 42	−3 63	−20 0	−2 0	1 3
cv23t	0 86	−2 18	−13 4	−2 2	2 0
cv25t	1 33	−2 55	−13 7	−2 2	2 8
cs18t	6 95	−4 78	−6 0	−23 6	2 7
csn8t	1 10	−1 03	−12 3	−19 9	2 8
cs28t	11 99	−11 13	−6 3	−25 3	2 2
csd8t	18 73	−17 76	−1 8	−29 8	1 7
cs23t	16 97	−15 54	−6 2	−20 2	2 6
cfn8t	0 24	−0 53	−6 4	−2 4	12 8
cf28t	1 31	−2 43	0 2	−2 6	18 8
cfd8t	1 98	−4 01	5 0	−2 7	23 9
cf23t	2 94	−4 55	9 0	−2 4	23 3
cf25t	4 35	−6 08	11 5	−1 7	26 2
ov28t	0 84	−2 07	−19 3	−2 5	1 7
os28t	11 61	−9 92	−7 6	−26 9	2 5
of28t	0 31	−1 32	−0 4	−2 4	21 1
cv28p	0 69	−1 99	−18 4	−2 3	1 6
cs28p	8 81	−10 08	−5 0	−30 1	2 4
cf28p	3 02	−3 59	1 7	−3 6	21 5
hs28g	114 4	−118 28	−3 5	−38 3	2 0
cs18g	38 69	−31 39	−4 6	−29 5	2 4
cs28g	44 60	−50 92	−4 1	−34 6	1 7
os28g	61.17	−66.22	7.6	−26.9	2.5

MASTER DE TÚNELES Y OBRAS SUBTERRÁNEAS

SIMULACIÓN NUMÉRICA

ARCILLAS EXPANSIVAS

TÚNELES IV Y V DEL SISTEMA DE TRASVASE DE LOS TÚNELES DEL SUR (TRASVASUR). GRAN CANARIA

PABLO DE LA FUENTE MARTÍN
DR. INGENIERO DE CAMINOS
UNIVERSIDAD POLITÉCNICA DE MADRID

TÚNELES IV Y V DE TRASVASUR

- COMIENZO TRABAJO DE PERFORACIÓN : 1.974.
- CAMPAÑAS DE RECONOCIMIENTO : 1974, 1986, 19
- PRESIÓN DE HINCHAMIENTO : P_H = 2-16 Kp/cm²
  HINCHAMIENTO LIBRE : 10%.-15%.
  W_L = 78 - 137 ; IP = 31-90
- ANÁLISIS DIFRACCIÓN RAYO X CONFIRMAN EL ELEVADO POTENCIAL EXPANSIVO (CONSTITUYENTE FUNDAMENTAL : ESMECTITA)
- EL HINCHAMIENTO AFECTÓ A SECCIONES PERFORADAS EN 1974 (DEFORMACIÓN DE LA SECCIÓN DE HORMIGÓN, LEVANTAMIENTO DEL FONDO)

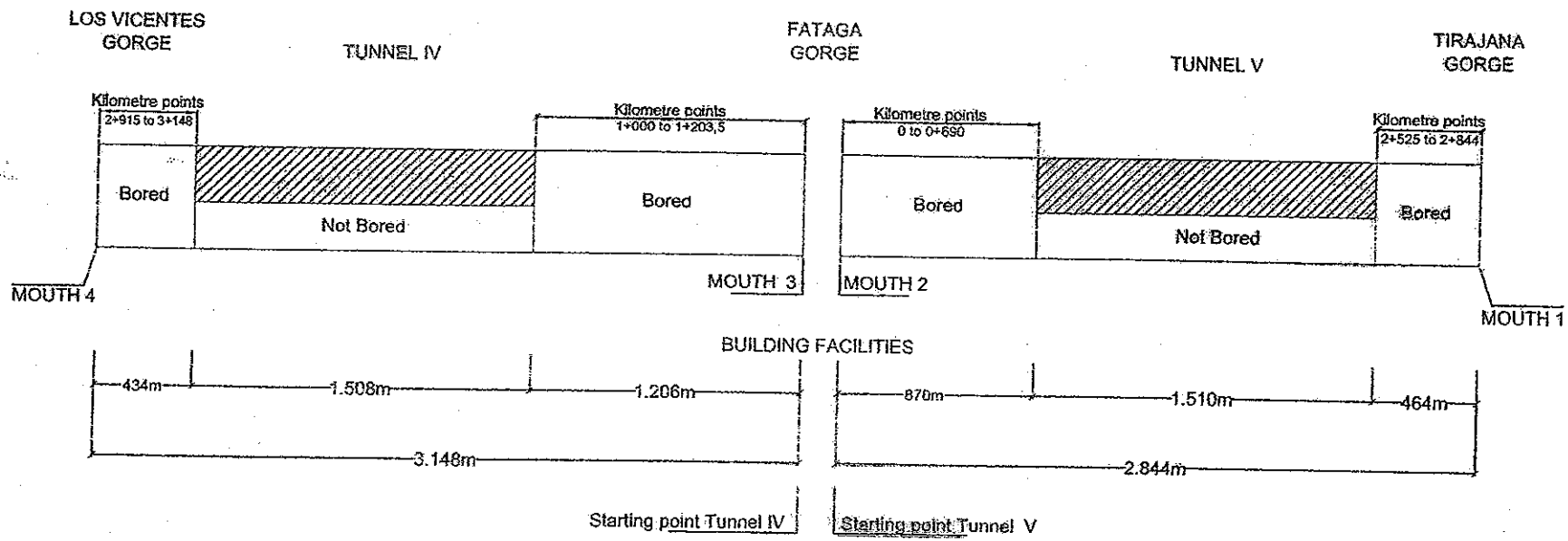

Fig. 1. State of the works when they were interrupted.

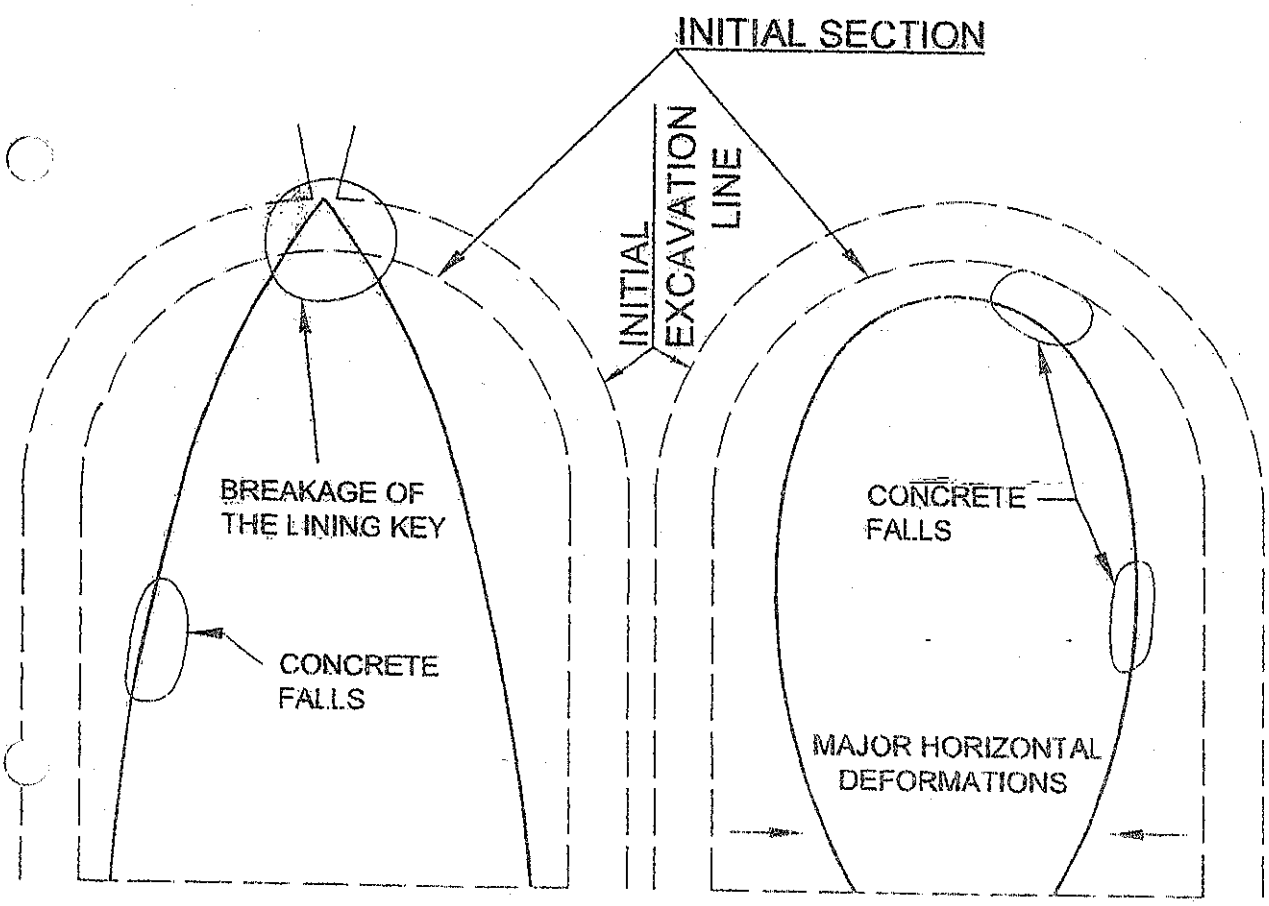

Fig. 3. Damage observed in tunnel IV.

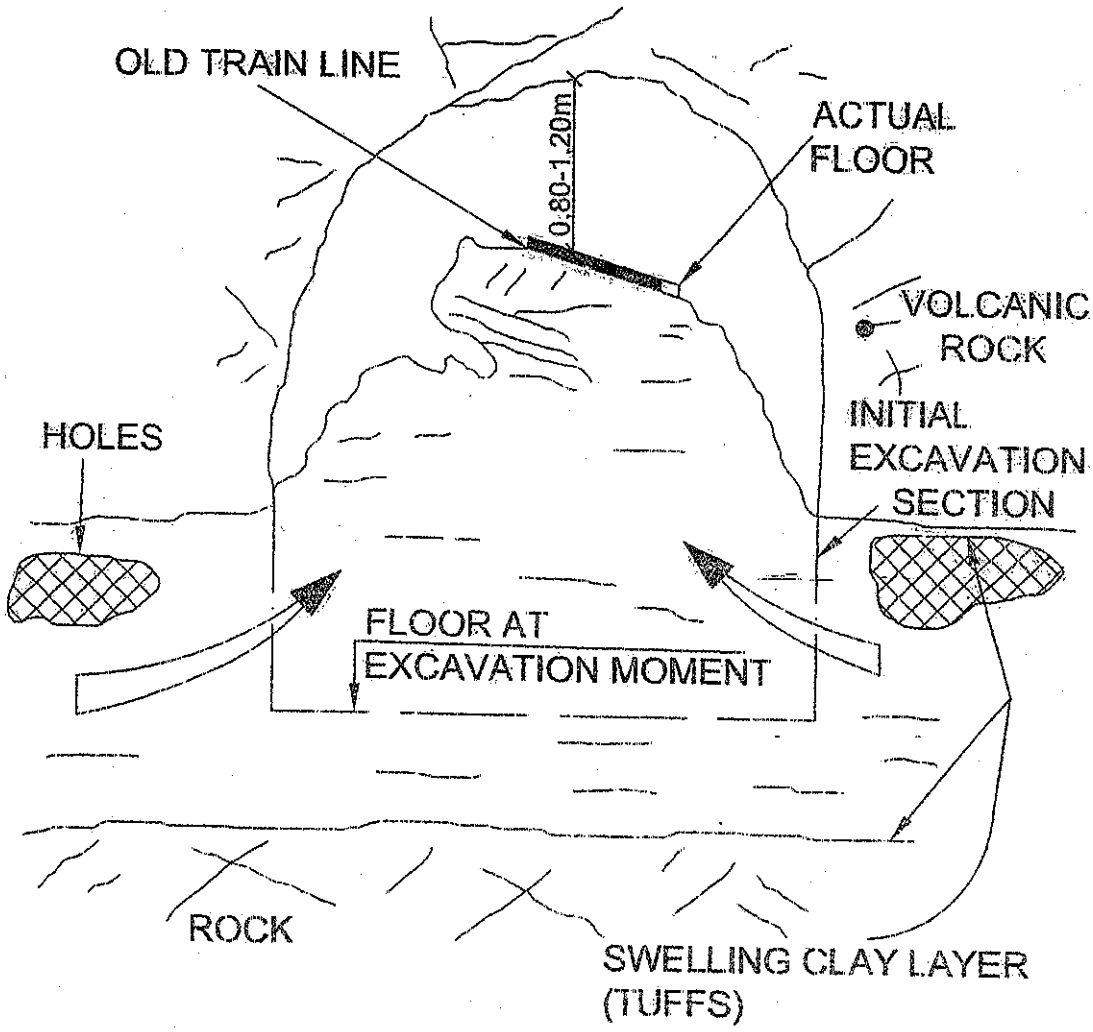

Fig. 5. Damage observed in tunnel V.

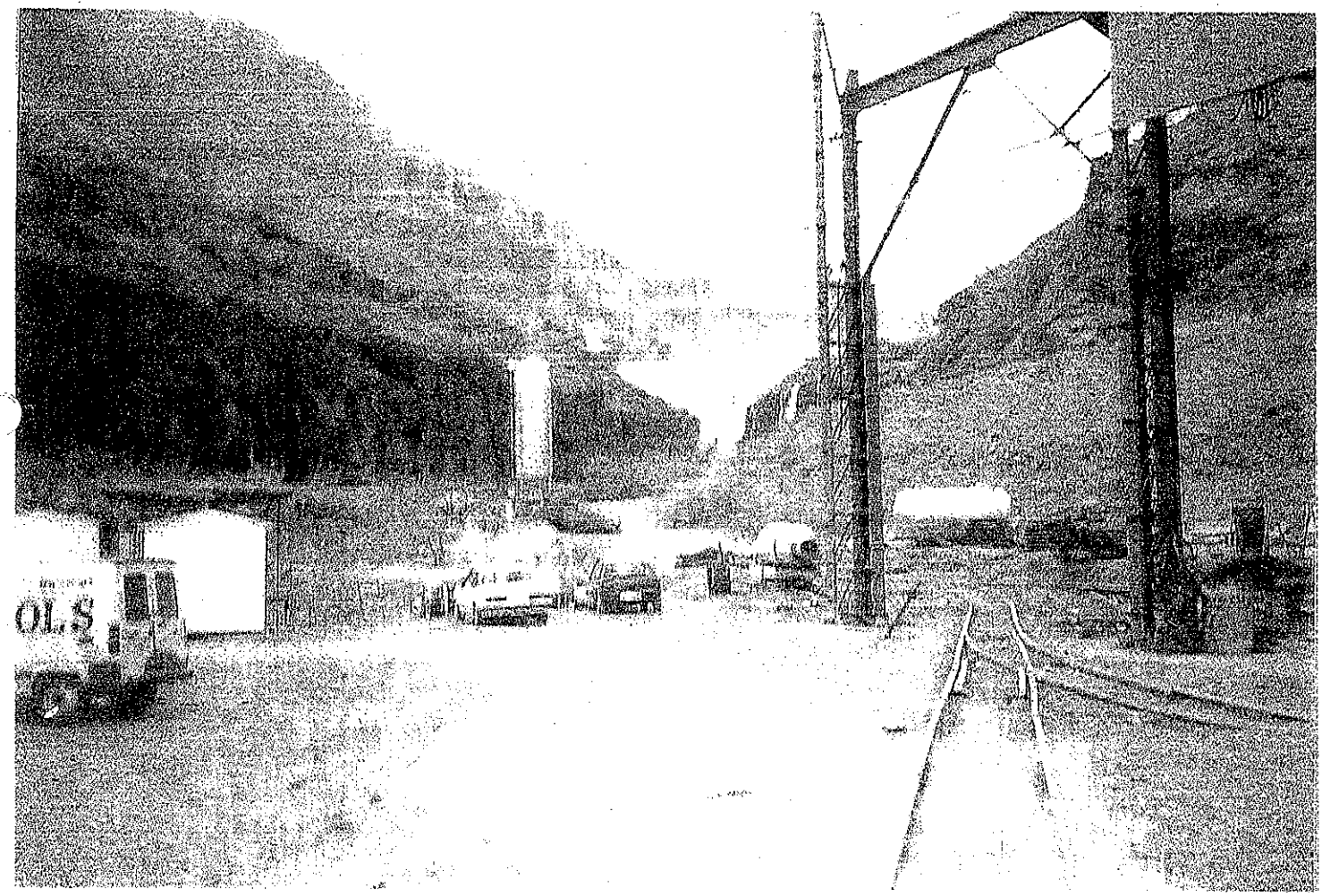
OLS

SCOUT

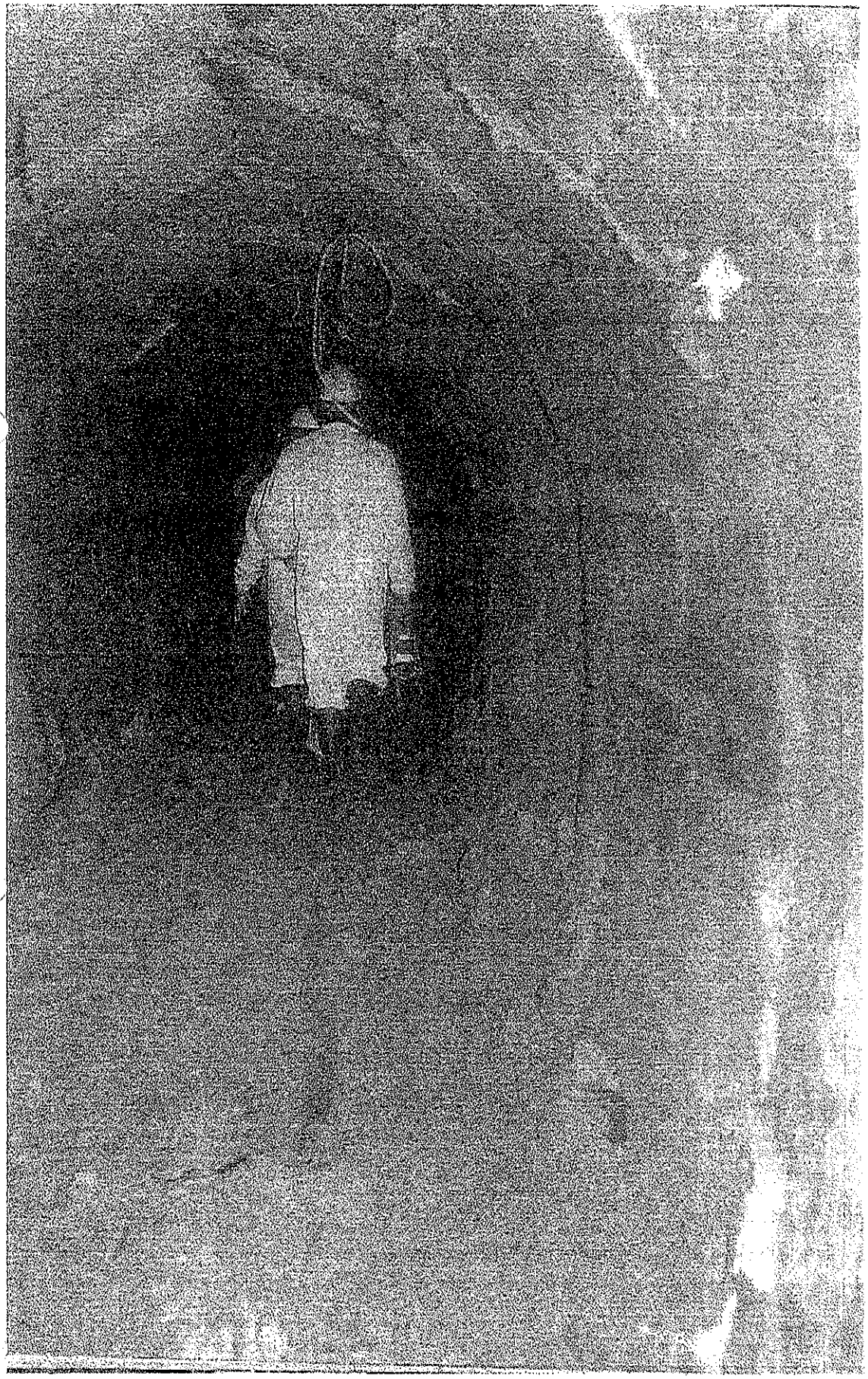

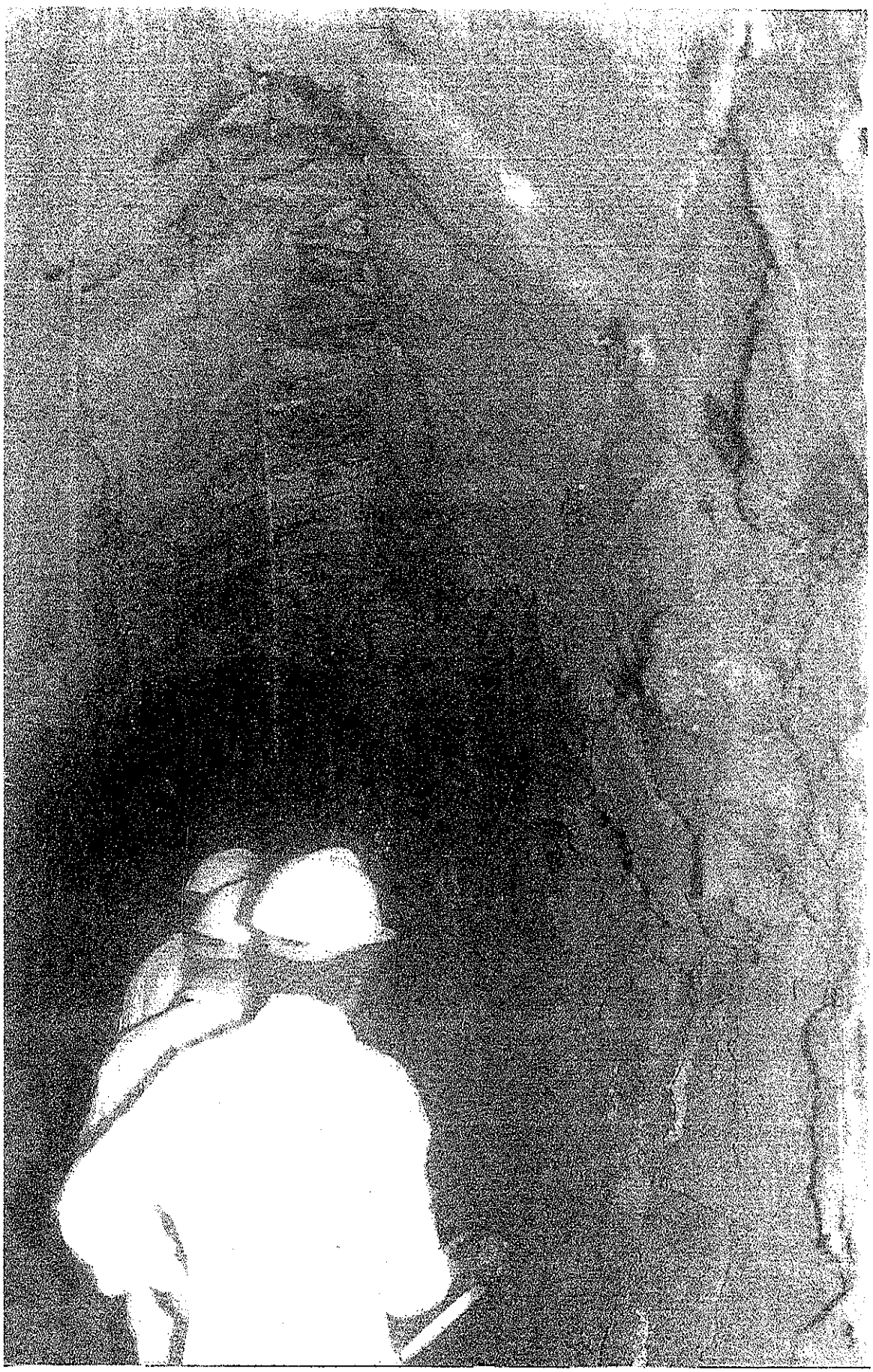

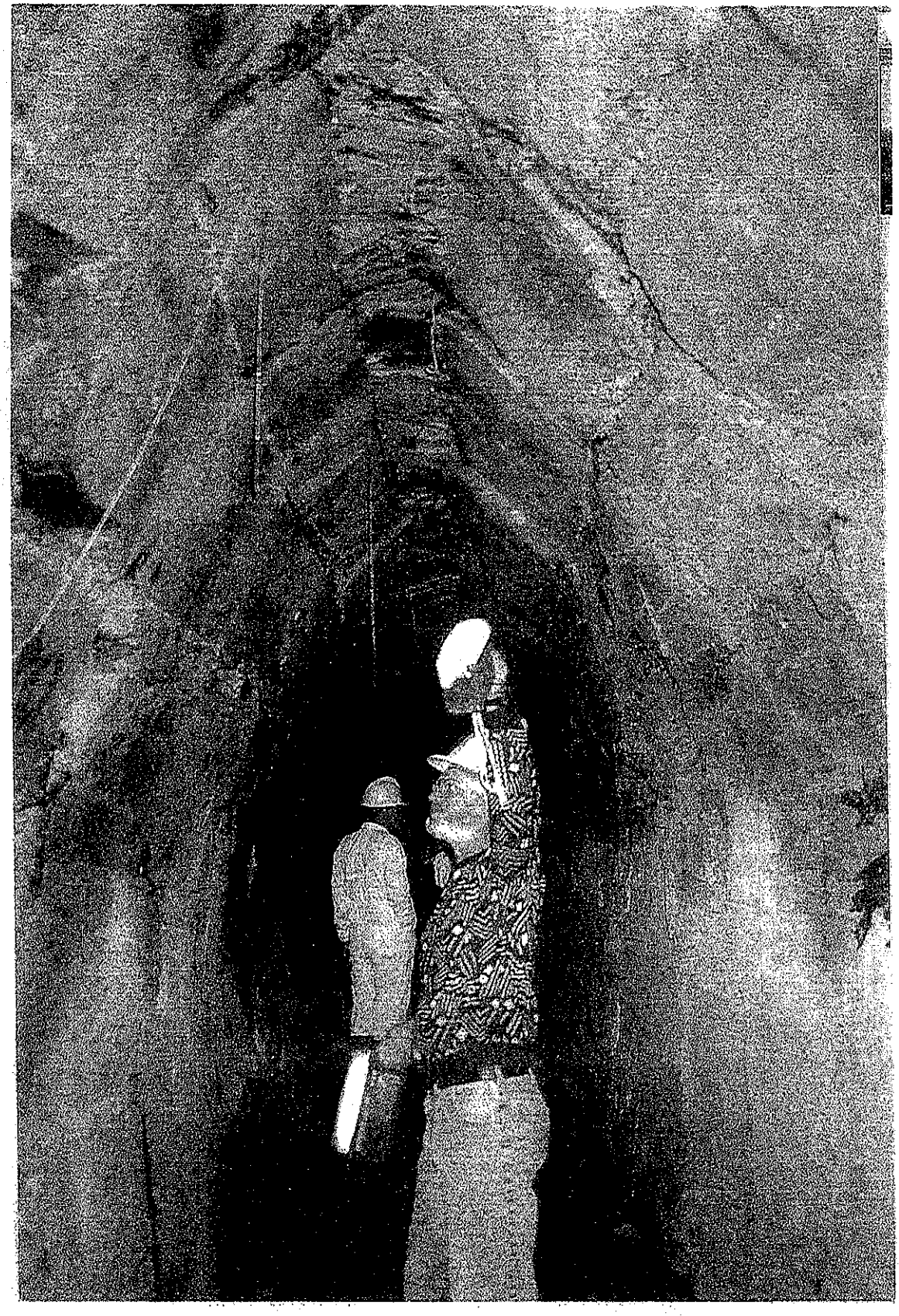

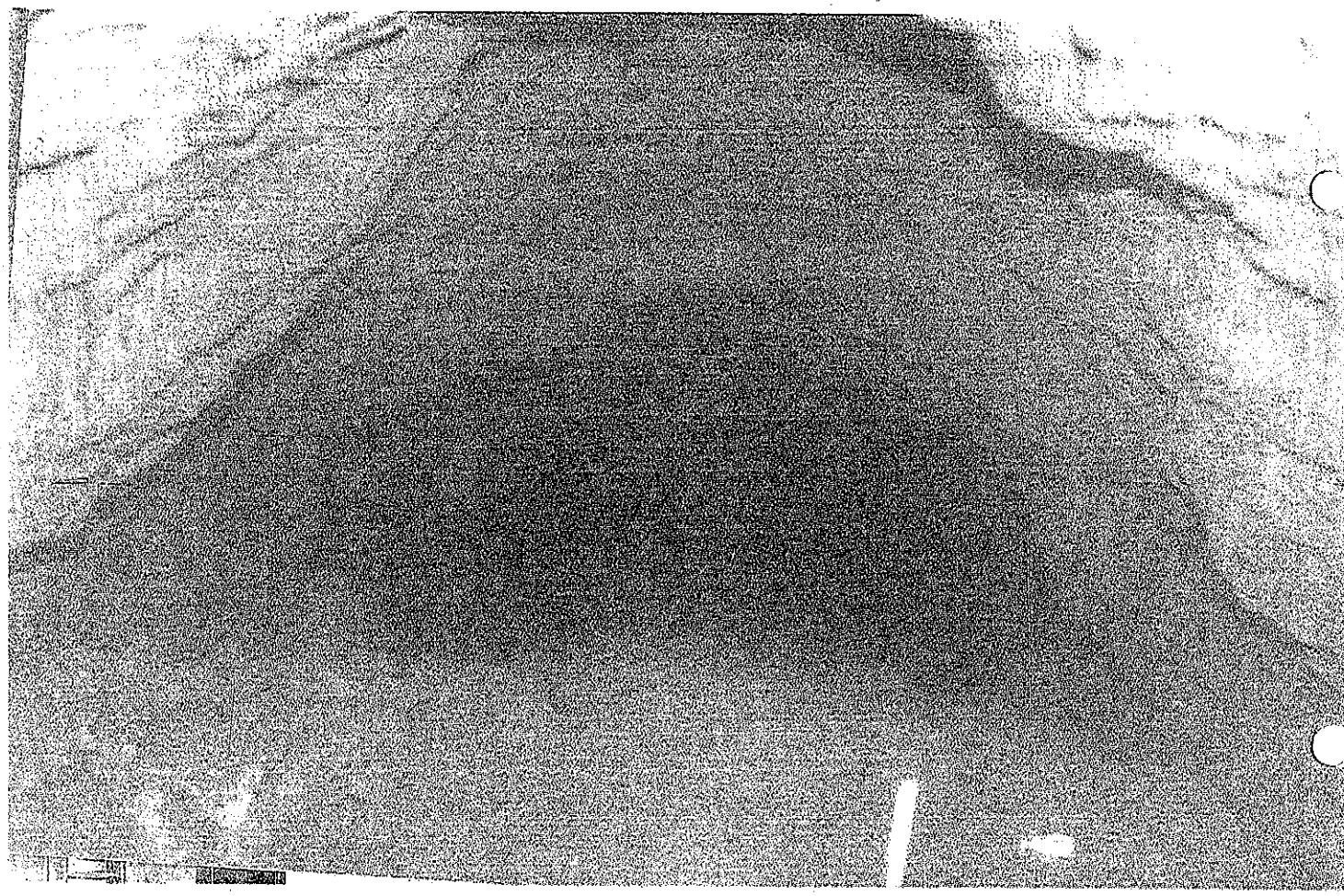

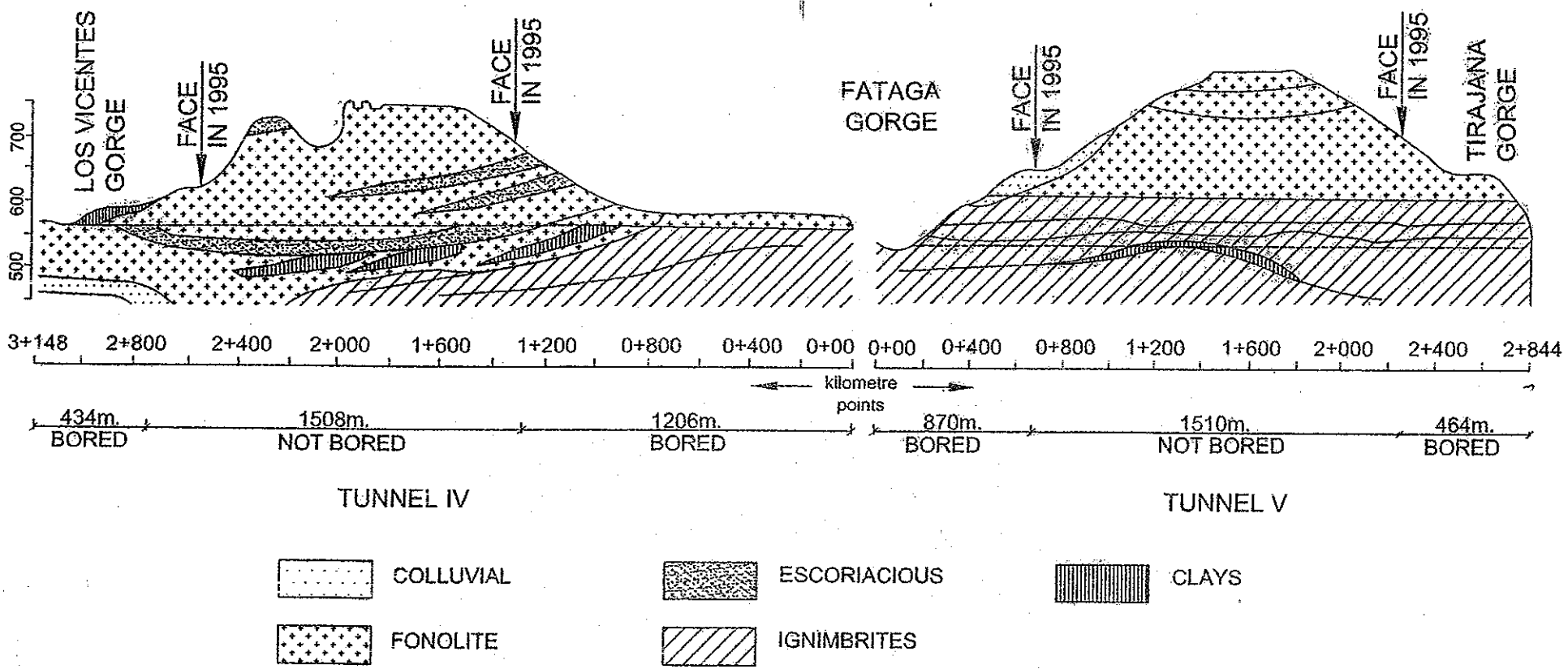

Fig. 7. Geological profile of tunnels IV and V.

Table 1
Index properties for samples from tunnels IV and V

Sample	Prospect	Tunnel	Kilometre point	Dry specific weight γ_d (kN/m^3)	Percentage of fines (%)	Water content in situ (%)	LL (%)	PL (%)	PI (%)	LI (%)	Sr (%)	USCS
MI-1	S2	IV	0+825	15.5	99	9	0	0	0	–	35	ML
MI-2	S4	IV	0+760	12.0	97	–	114	44	70	–	–	CH
MI-3	S4	IV	0+760	12.9	100	4	137	47	90	−0.5	8	CH
MI-4	S4	IV	0+760	13.2	99	34	129	56	73	−0.3	91	MH
MI-5	S4	IV	0+760	15.5	100	24	115	48	67	−0.4	92	MH
MI-6	S6	V	0+645	–	100	–	84	48	36	–	–	MH
MI-7	S6	V	0+645	–	100	–	86	45	41	–	–	MH
MI-8	S6	V	0+645	–	99	–	85	48	37	–	–	MH
MI-9	S5	V	0+675	19.6	92	–	54	23	31	–	–	CH
MA-1	–	IV	0+820	10.0	91	64	208	44	164	0.1	100	CH
MA-2	–	IV	0+814	10.2	90	60	198	49	149	0.1	100	CH
MA-3	–	IV	0+805	13.3	36	21	79	38	41	−0.4	57	MH
MA-4	–	V	0+685	13.6	64	27	78	29	49	0.0	77	CH
MA-5	–	V	0+698	10.5	94	51	103	45	58	0.1	90	MH
MA-6	–	V	0+705	15.8	30	25	79	28	51	−0.1	98	GC

q_u = 4 – 12 kp/cm² (en zonas de arcilla no alteradas)

$q_u \simeq 0.3$ kp/cm² (en zonas próximas a la excavación)

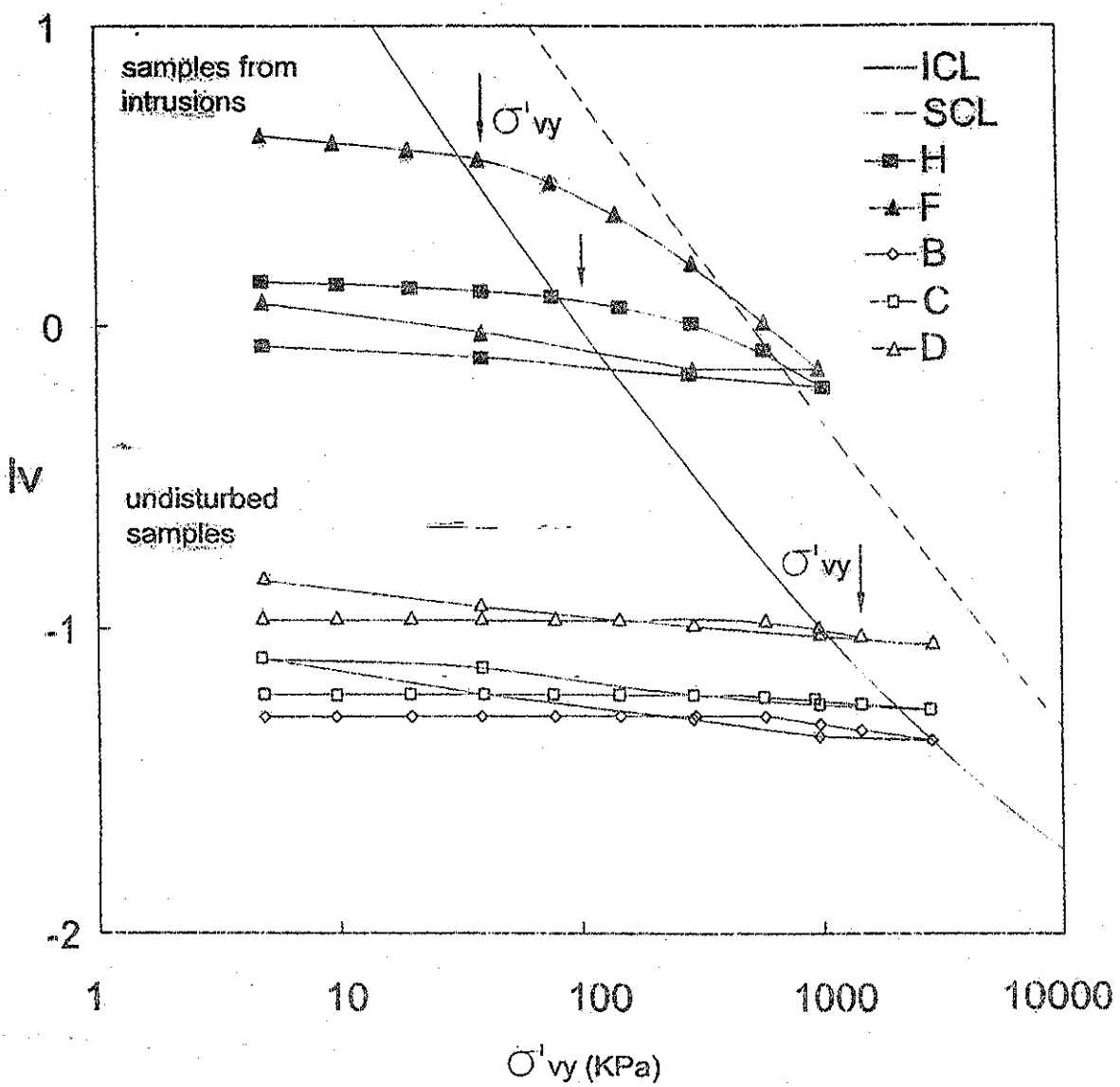

Fig. 9. Oedometric tests of expansive clay samples.

PRIMER ESTUDIO (1994)

- SE ANALIZARON TRES SECCIONES.
  - SECCIÓN DE PROYECTO
  - SECCIÓN OVALADA
  - SECCIÓN CIRCULAR

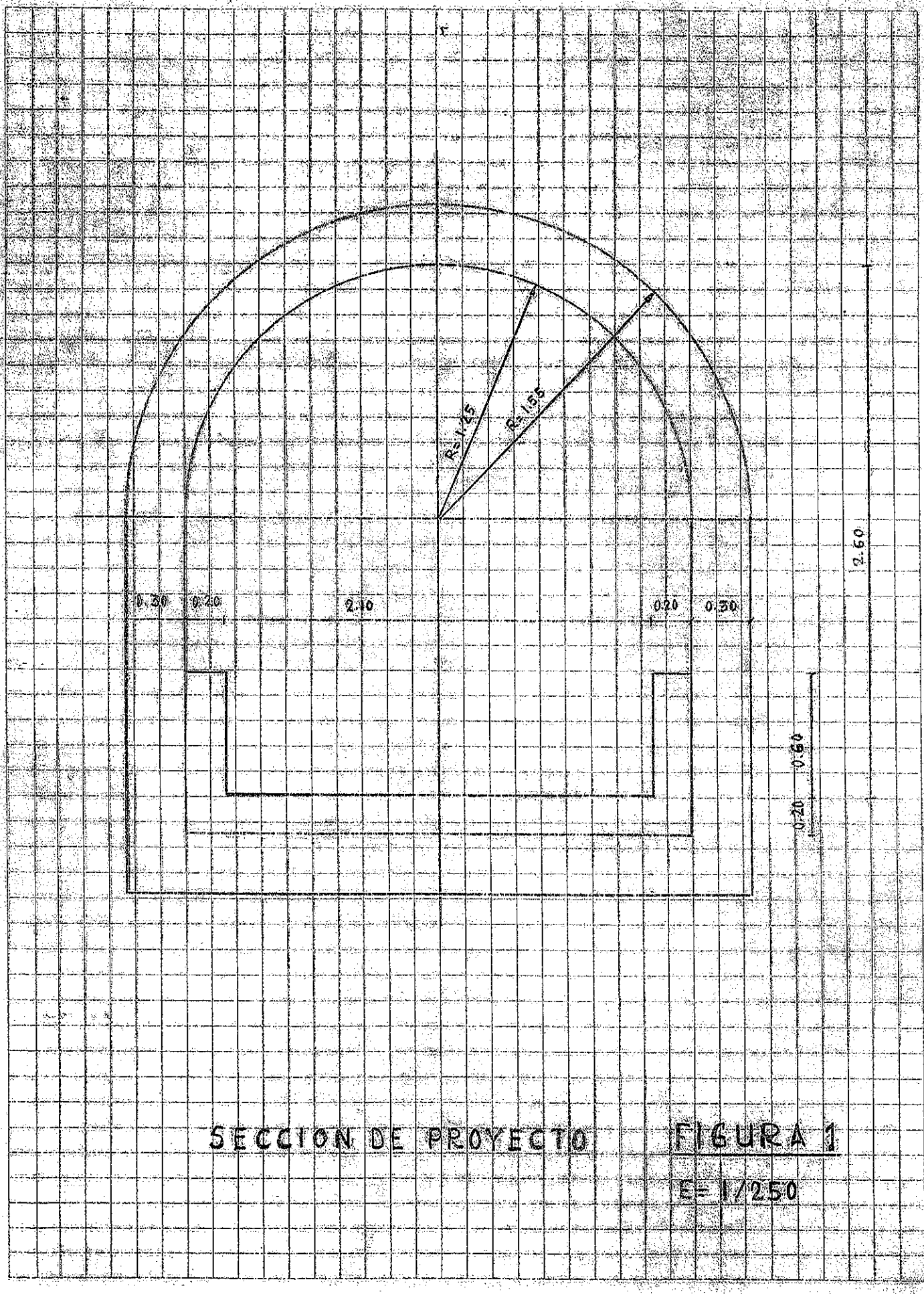

SECCION DE PROYECTO

FIGURA 1

E= 1/250

SECCION OVALADA

FIGURA 2

E= 1/250

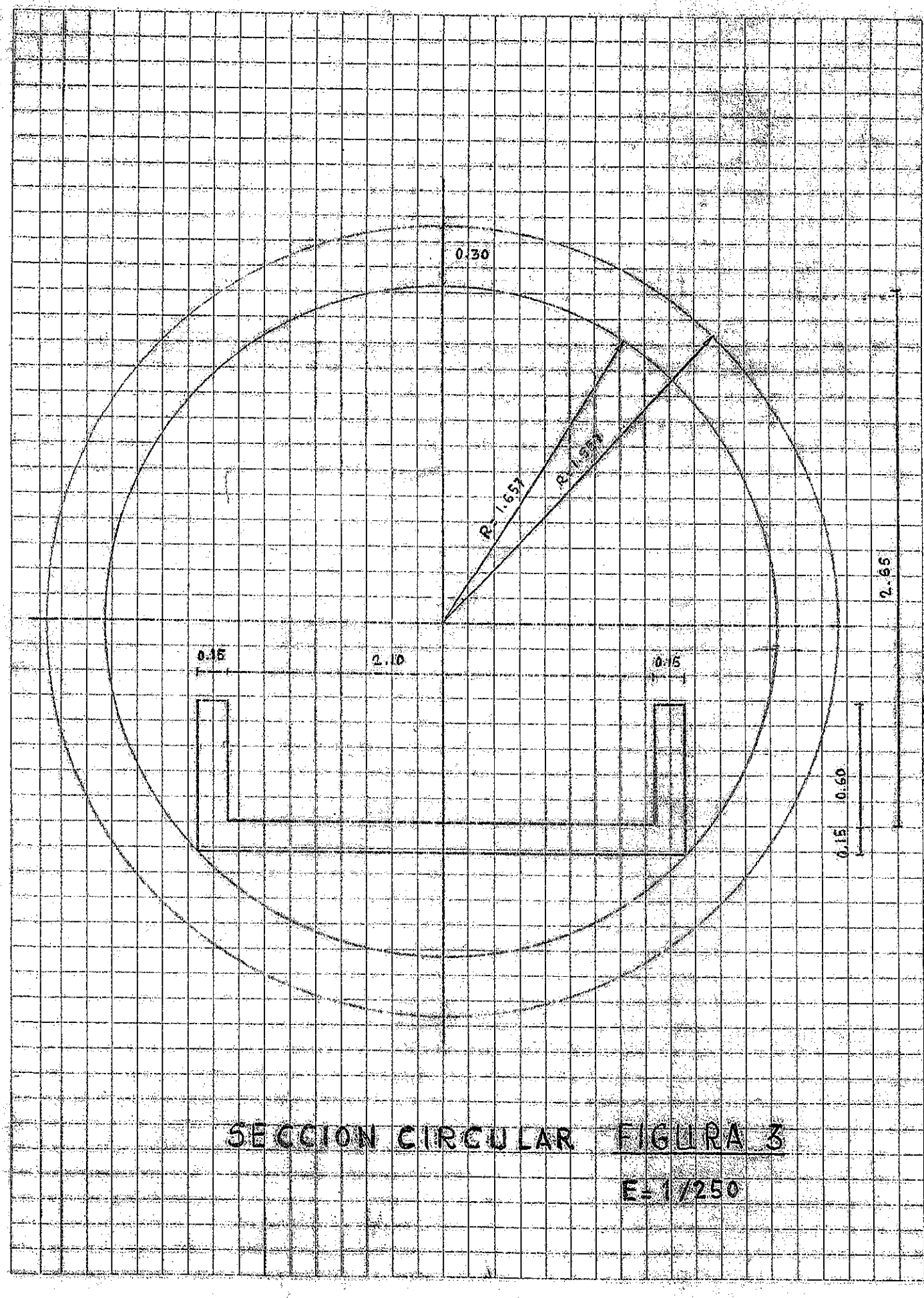

SECCION CIRCULAR FIGURA 3

E=1/250

MODELO DE CÁLCULO. ACCIONES

- MODELO EN 2D (DEFORMACIÓN PLANA)

- TERRENO: CUADRILÁTEROS DE 8 NODOS
  TRIÁNGULOS DE 6 NODOS
  (2 GDL / NODO)

  REVESTIMIENTO: ELEMENTO VIGA DE 2 NODOS
  (3 GDL / NODO)

- EN LAS SECCIONES DE PROYECTO Y OVALADA SE CONSIDERÓ EL ESTADO CORRESPONDIENTE A UN INCREMENTO DE VOLUMEN.

- EN LA SECCIÓN CIRCULAR, ADEMÁS DEL INCREMENTO DE VOLUMEN SE TUVO EN CUENTA LA ACCIÓN DEL TERRENO SOBRE EL REVESTIMIENTO.

SIMULACIÓN DEL INCREMENTO DE VOLUMEN MEDIANTE UN INCREMENTO DE TEMPERATURA

$$\begin{Bmatrix} \varepsilon_x \\ \varepsilon_y \\ \varepsilon_z \\ 2\varepsilon_{xy} \\ 2\varepsilon_{yz} \\ 2\varepsilon_{zx} \end{Bmatrix} = \frac{1}{E} \begin{bmatrix} 1 & -\nu & -\nu & 0 & 0 & 0 \\ -\nu & 1 & -\nu & 0 & 0 & 0 \\ -\nu & -\nu & 1 & 0 & 0 & 0 \\ 0 & 0 & 0 & 2(1+\nu) & 0 & 0 \\ 0 & 0 & 0 & 0 & 2(1+\nu) & 0 \\ 0 & 0 & 0 & 0 & 0 & 2(1+\nu) \end{bmatrix} \begin{Bmatrix} \sigma_x \\ \sigma_y \\ \sigma_z \\ \tau_{xy} \\ \tau_{yz} \\ \tau_{zx} \end{Bmatrix} + \alpha_x T \begin{Bmatrix} 1 \\ 0 \\ 0 \\ 0 \\ 0 \\ 0 \end{Bmatrix} + \alpha_y T \begin{Bmatrix} 0 \\ 1 \\ 0 \\ 0 \\ 0 \\ 0 \end{Bmatrix} + \alpha_z T \begin{Bmatrix} 0 \\ 0 \\ 1 \\ 0 \\ 0 \\ 0 \end{Bmatrix}$$

EN DEFORMACIÓN PLANA:

$$\varepsilon_z = \varepsilon_{zx} = \varepsilon_{zy} = 0$$

$$\begin{Bmatrix} \varepsilon_x \\ \varepsilon_y \\ 2\varepsilon_{xy} \end{Bmatrix} = \frac{1+\nu}{E} \begin{bmatrix} (1-\nu) & -\nu & 0 \\ -\nu & (1-\nu) & 0 \\ 0 & 0 & 2 \end{bmatrix} \begin{Bmatrix} \sigma_x \\ \sigma_y \\ \tau_{xy} \end{Bmatrix} + T \begin{bmatrix} \nu\alpha_z + \alpha_x \\ \nu\alpha_z + \alpha_y \\ 0 \end{bmatrix}$$

$V_0 = l_{0x} \cdot l_{0y} \cdot l_{0z}$ (volumen de un hexaedro)

Si $l_{0z} = 0$

$V_0 + \Delta V_0 = (l_{0x} + \Delta l_{0x})(l_{0y} + \Delta l_{0y}) \cdot l_{0z}$

$\Delta V_0 = l_{0x} \cdot l_{0z} \cdot \Delta l_{0y} + l_{0y} \cdot l_{0z} \cdot \Delta l_{0x} + l_{0z} \Delta l_{0x} \cdot \Delta l_{0y}$

$$\varepsilon = \frac{\Delta V_0}{V_0} = \frac{\Delta l_{0y}}{l_{0y}} + \frac{\Delta l_{0x}}{l_{0x}} + \frac{\Delta l_{0x} \cdot \Delta l_{0y}}{l_{0x} l_{0y}} =$$

$$= T(\nu\alpha_z + \alpha_y) + T(\nu\alpha_z + \alpha_x) + T^2(\nu\alpha_z + \alpha_y)(\nu\alpha_z + \alpha_x)$$

Con $\alpha_x = \alpha_y = \alpha_z = \alpha$

$$\underline{\varepsilon = 2T\alpha(1+\nu)}$$

$\varepsilon = 0.5\% - 3\%$ (HINCHAMIENTO LIBRE: $10\% - 15\%$)

FIJADO $\alpha \rightarrow T$

3% 0.5%

0 0.5 1.0 1.5 2.0 2.5

ALREDEDOR TÚNEL

EN SECCIONES OVALADA Y CIRCULAR TAMBIÉN EN CAPA DE 1.5 M DE ESPESOR EN HASTIALES

- PARÁMETROS ELÁSTICOS:

SUELO ARCILLOSO: $E = 600\ kp/cm^2$; $\nu = 0.3$

SUELO MARGINOSO: $E = 15.000\ kp/cm^2$; $\nu = 0.25$.

SECCIÓN DE PROYECTO

ESFUERZOS EN EL REVESTIMIENTO (0.30M)

VCAN 1

INCREMENTO DE VOLUMEN ALREDEDOR DE LA CAVIDAD.

0.5% A 2M ; 3% A 0.5M.

$\sigma = (15 \pm 137)\ kp/cm^2$

TRACCIÓN $> 120\ kP/cm^2$.

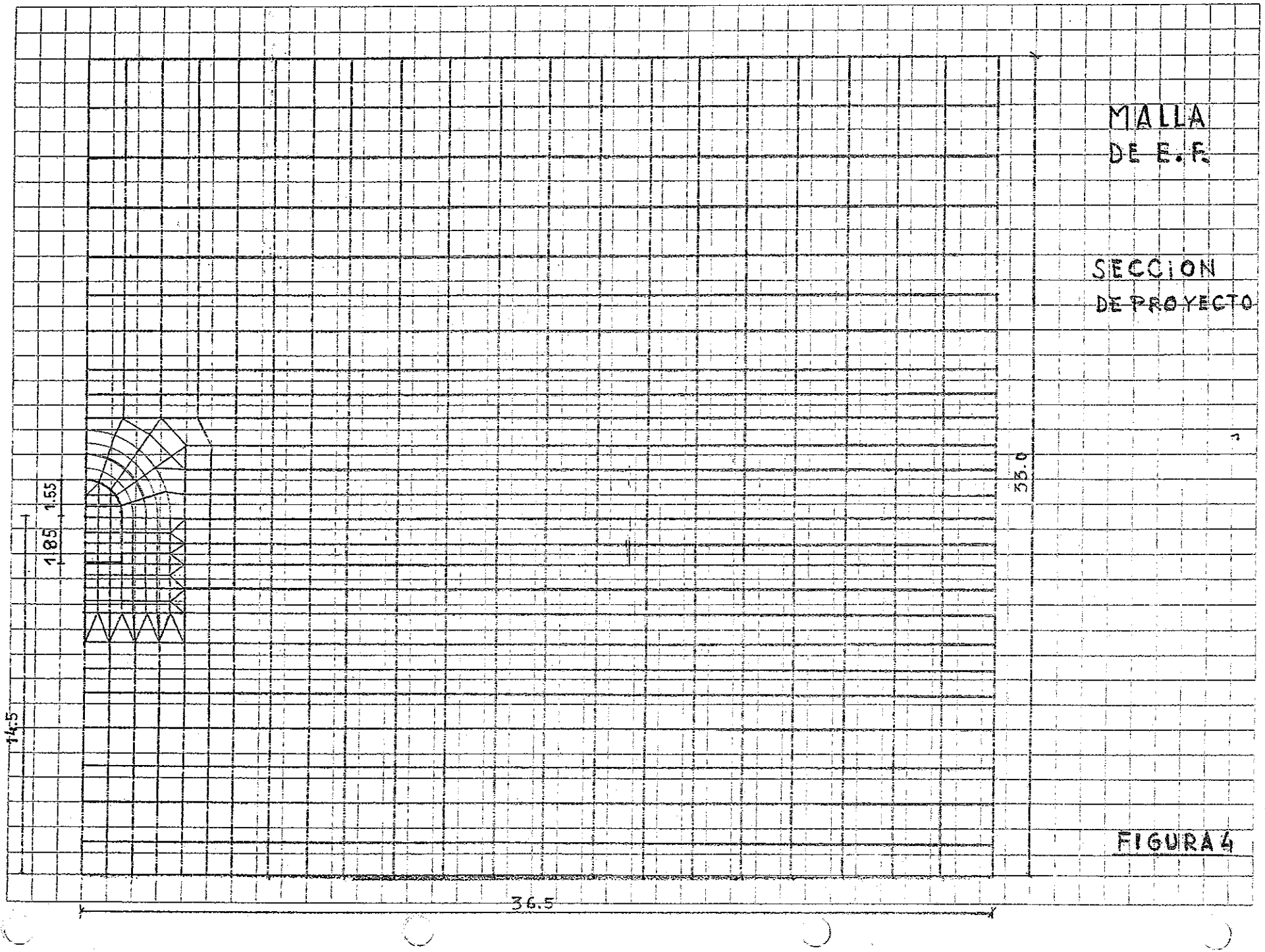

FIGURA 4

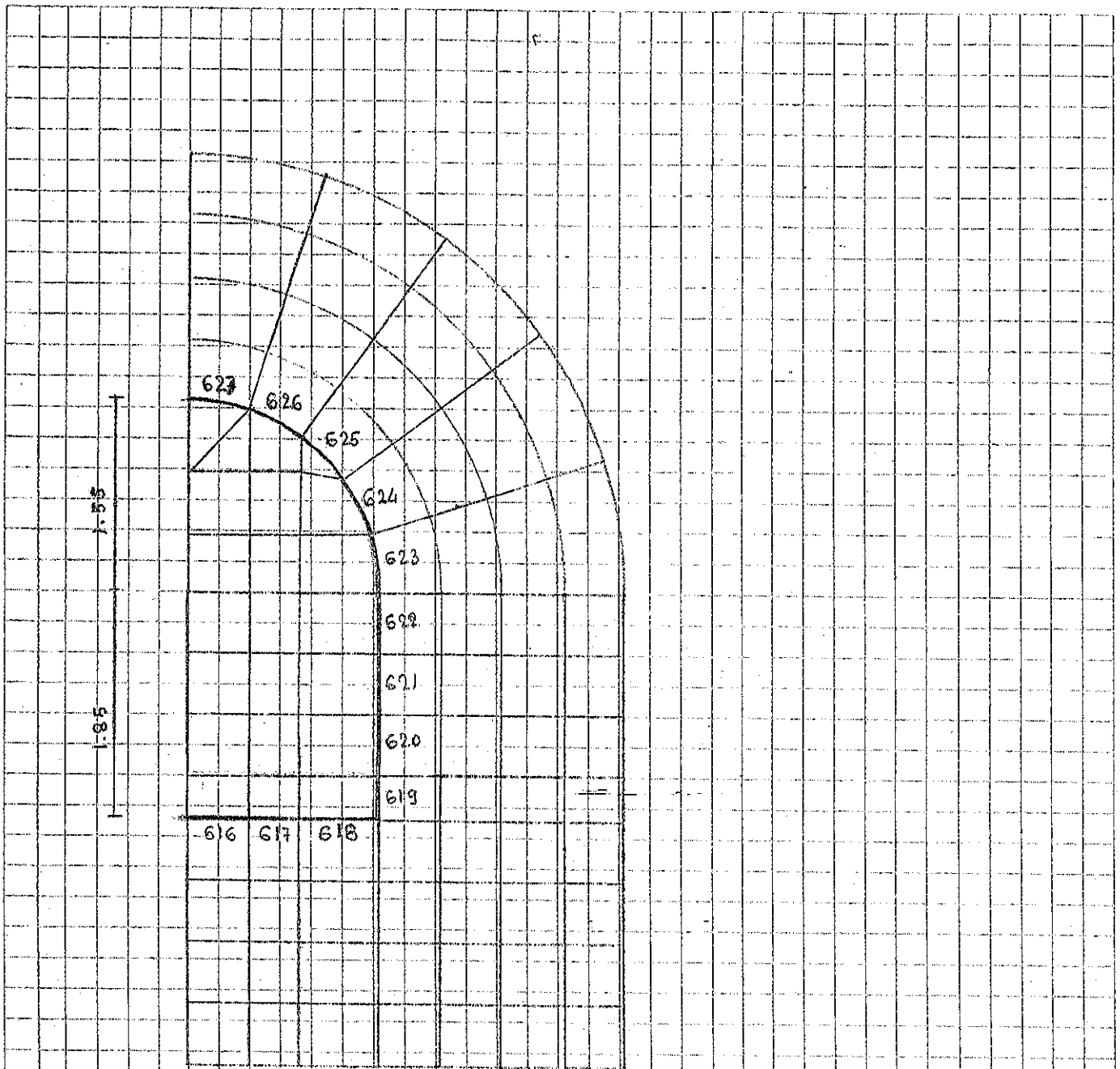

DETALLE DE LA MALLA DE E. F.

SECCION DE PROYECTO

FIGURA 4.A

SECCIÓN OVALADA
ESFUERZO EN LA SECCIÓN (0.30 M)

VCAN 2

VCAN 3 ‖ SE ANALIZA LA INFLUENCIA DE LA
VCAN 4 ‖ RESTRICCIÓN DE LOS BORDES SUPERIOR E INFERIOR DE LA MALLA.

INCREMENTO DE VOLUMEN ALREDEDOR DE LA CAVIDAD DEL 2% ENTRE 0.5 M Y 2.5 M

ESFUERZOS SIMILARES: $\sigma = (58.5 \pm 156)$ kp/cm²

TRACCIÓN ≤ 100 kp/cm²

VCAN 5 : INCREMENTO DE VOLUMEN ALREDEDOR DE LA CAVIDAD.

3% A 0.5 M ; 0.5% A 2 M.

$\sigma = (37.5 \pm 104.5)$ kp/cm²

TRACCIÓN ≤ 67 kp/cm²

VCAN 6 : INCREMENTO DE VOLUMEN EN CAPA DE 1.5 M EN HASTIALES

2% A 0.5 M (EN CENTRO CAPA)

0.5% A 0.7 M (AL ALEJARSE DEL CENTRO DE CAPA)

0.5% A 2.0 M.

$\sigma = (-2.5 \pm 94.5)$ kp/cm²

TRACCIÓN ≤ 97 kp/cm²

≃1.2m

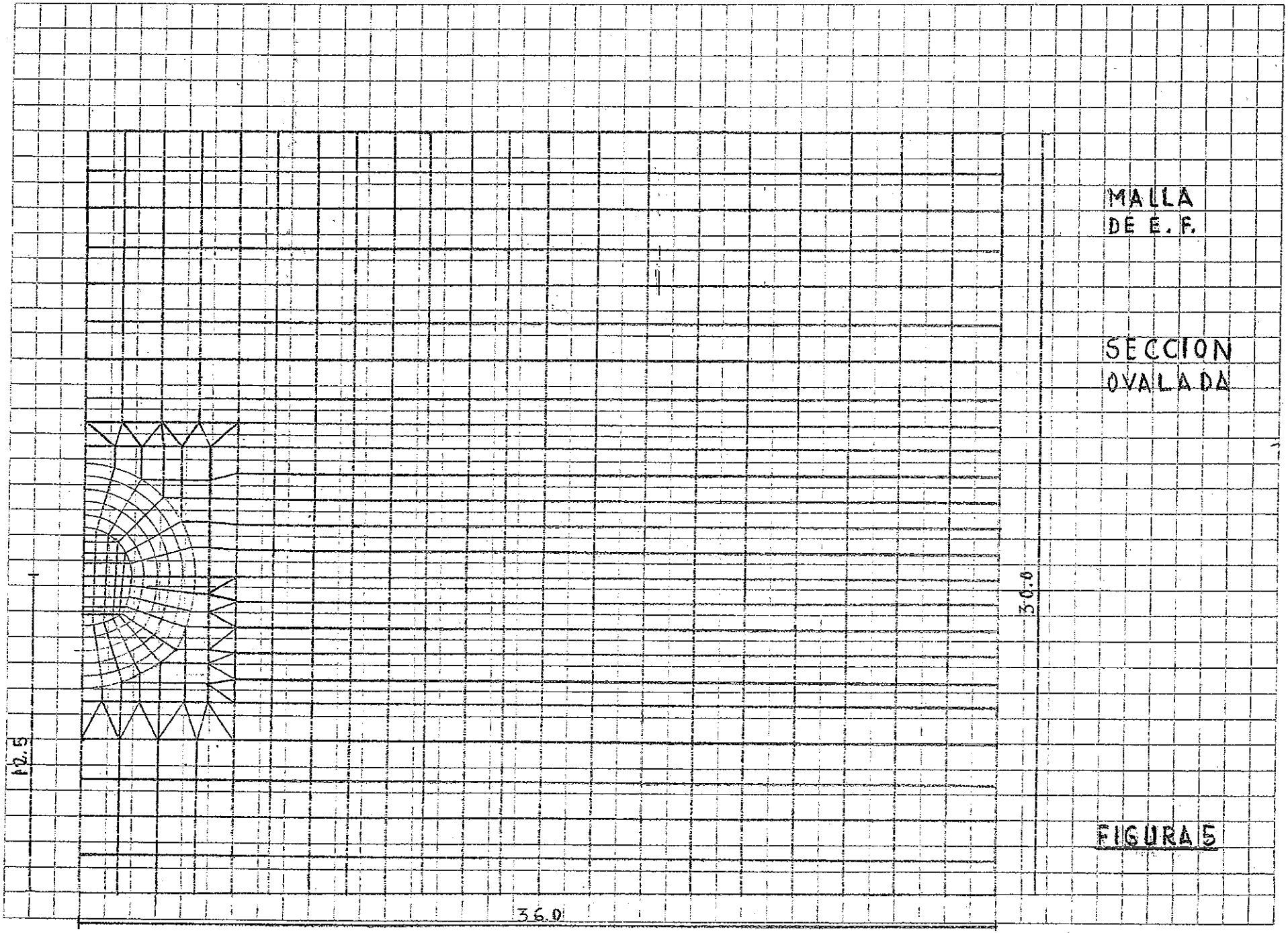

FIGURA 5

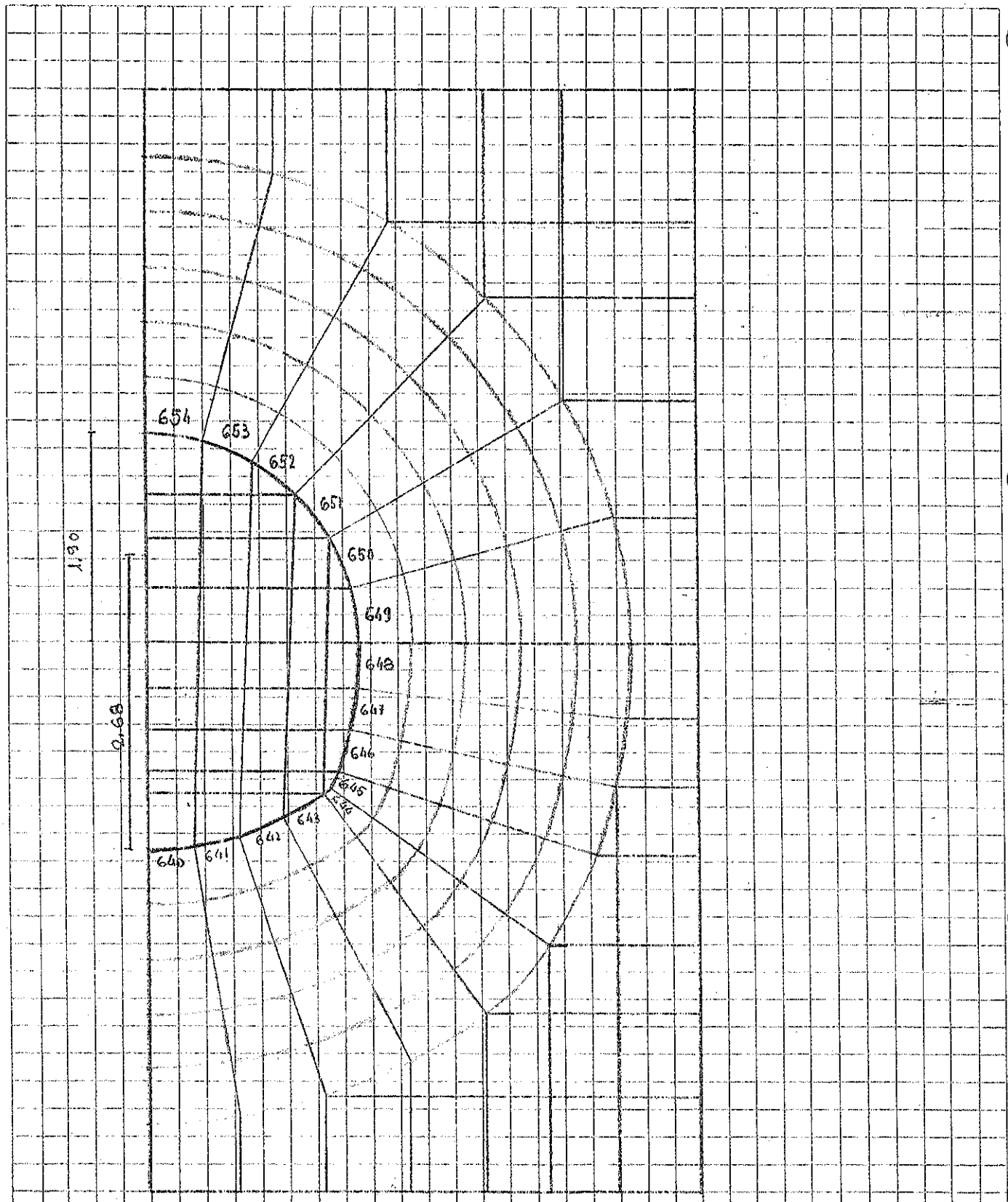

DETALLE DE LA MALLA DE E.F.

SECCION OVALADA

FIGURA 5.A

SECCIÓN CIRCULAR

ESFUERZO EN EL REVESTIMIENTO (0.30 M)

ECAN 7 ‖ SE ANALIZAN ESFUERZO ORIGINADO
ECAN 8 ‖ POR LA EXCAVACIÓN.

(DIFINIR RECUBRIMIENTO)

COMPRESIÓN ≤ 16 kp/cm²
TRACCIÓN ≤ 10 kp/cm².

VCAN 9 (RECUBRIMIENTO, 18 M)

VCAN 10 (RECUBRIMIENTO, 30 M)

INCREMENTO DE VOLUMEN ALREDEDOR DE LA CAVIDAD : 3% A 0.5 M.
0.5% A 2 M.

$\sigma \simeq (36 \pm 1)$ kp/cm²

NO HAY TRACCIONES.

VCAN 11 : INCREMENTO DE VOLUMEN EN CAPA DE 1.5 M ENTRE ALETAS

2% A 0.5 M (EN CENTRO CAPA)
0.5% A 0.5 M (EN ALETAS DE CENTRO CAPA)
0.5% A 2 M.

$\sigma = (-1 \pm 69{,}5)$ kp/cm²

TRACCIÓN ≤ 7 kp/cm² (25% INFERIOR A LA DE SECCIÓN OVALADA)

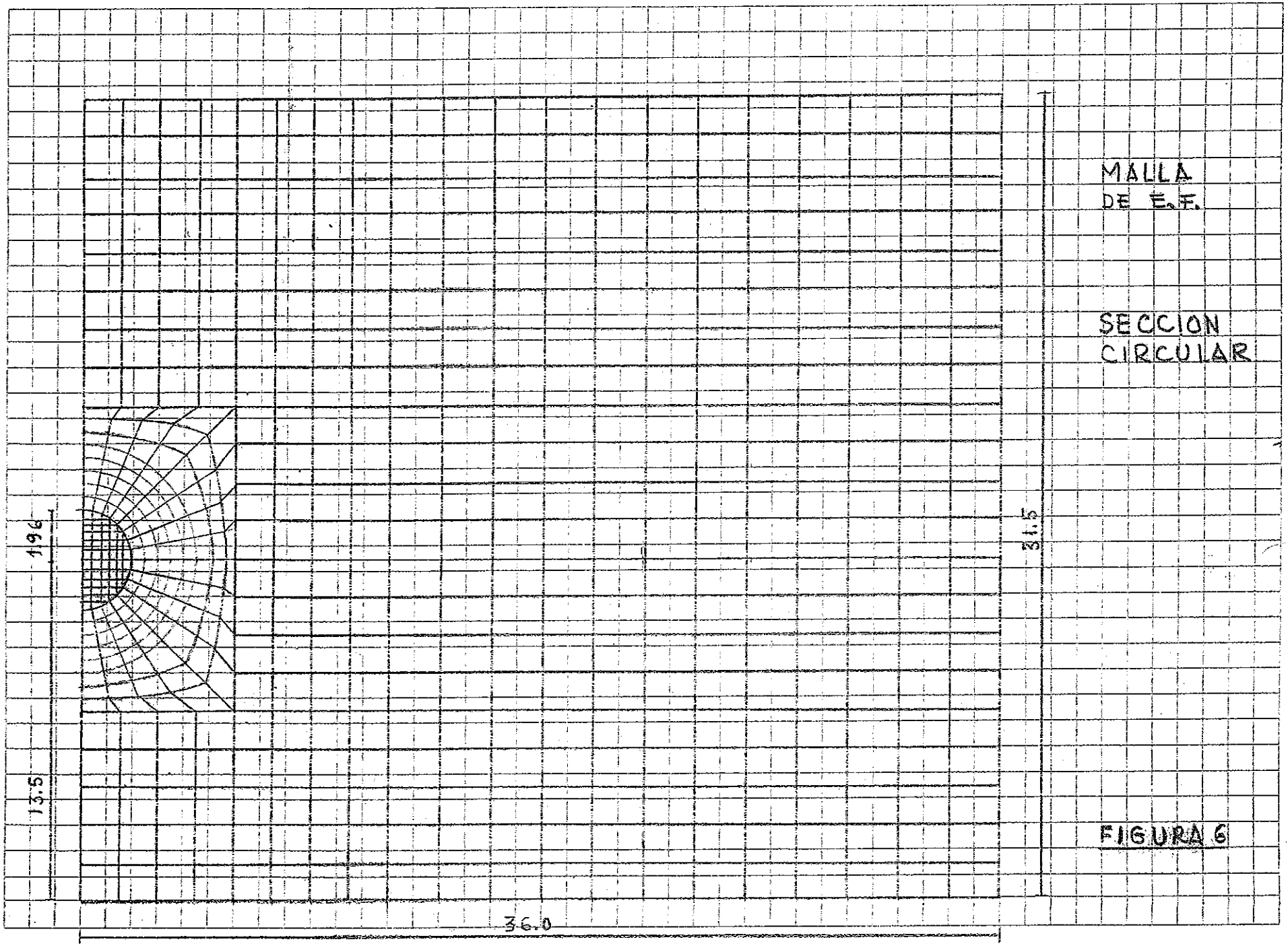

FIGURA 6

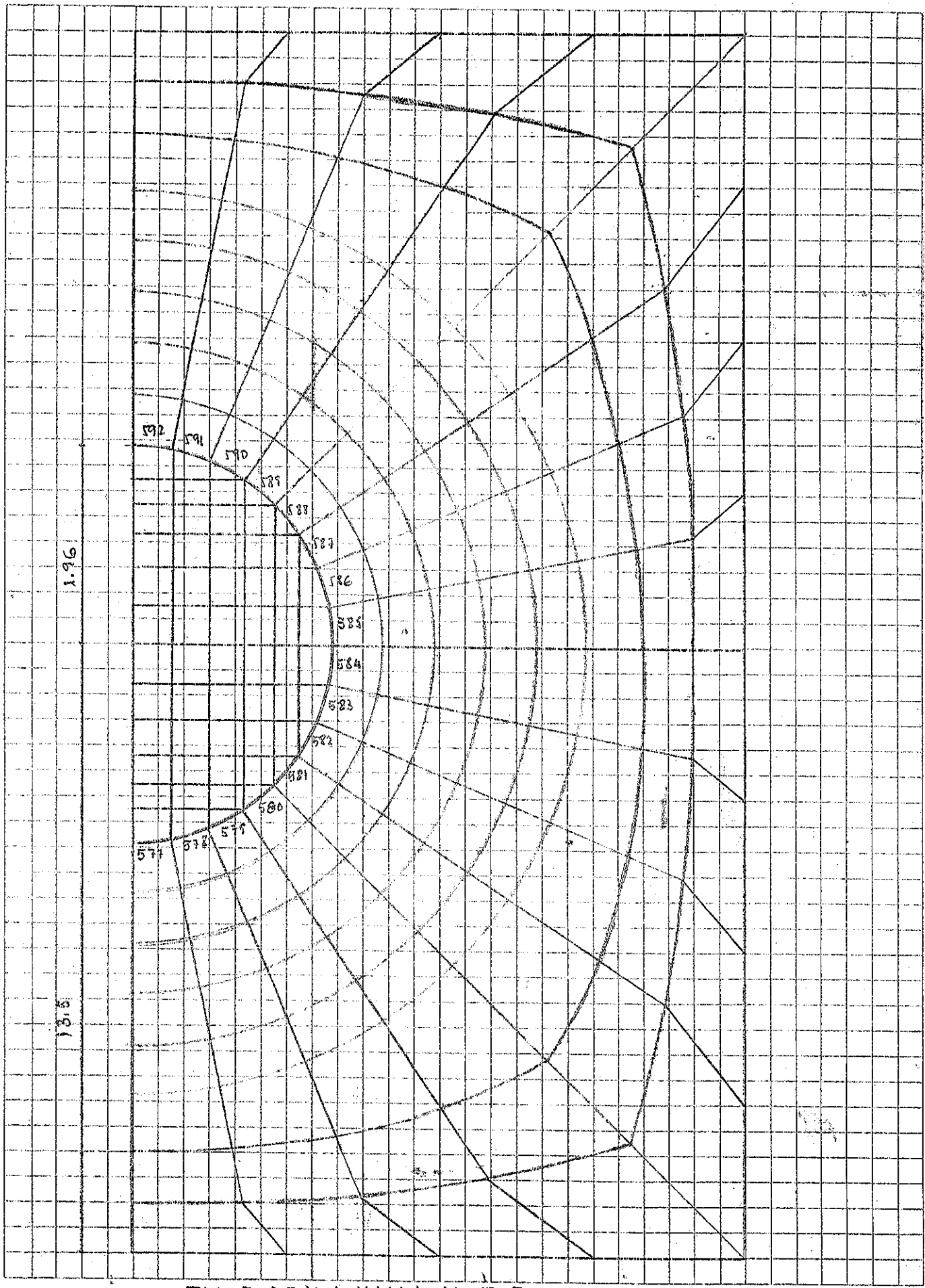

DETALLE DE LA MALLA DE E.F.
SECCION CIRCULAR

FIGURA 6.A

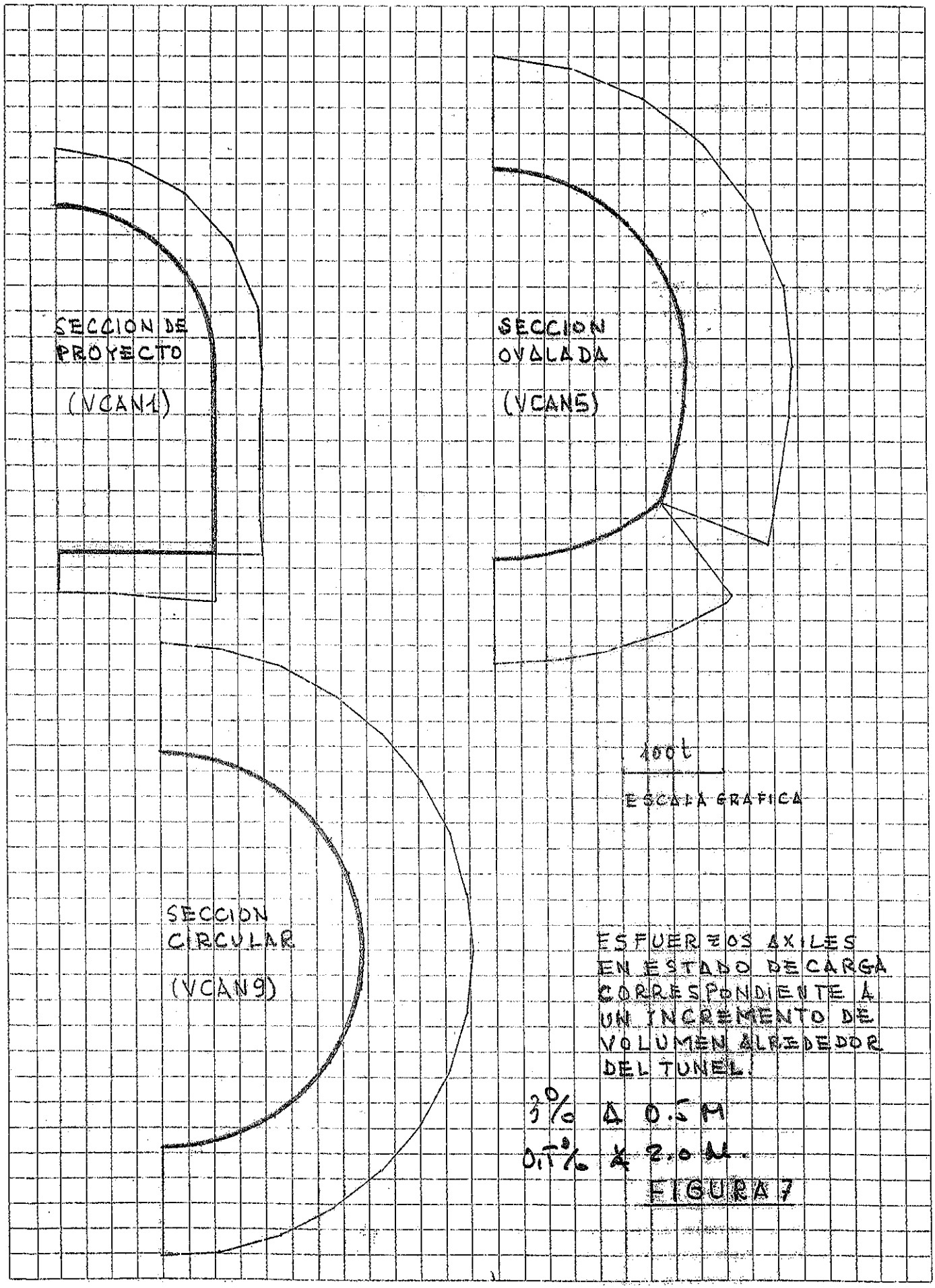
SECCION DE PROYECTO
(VCAN1)
SECCION OVALADA
(VCAN5)
SECCION CIRCULAR
(VCAN9)
100 L
ESCALA GRAFICA
ESFUERZOS AXILES EN ESTADO DE CARGA CORRESPONDIENTE A UN INCREMENTO DE VOLUMEN ALREDEDOR DEL TUNEL:
3% Δ 0.5 M
0.1% Δ 2.0 M.

FIGURA 7

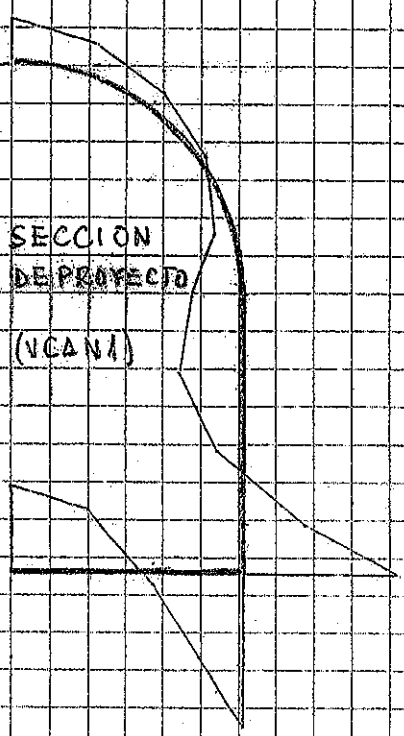

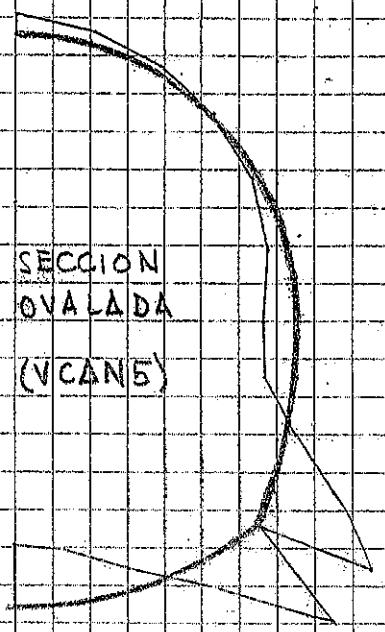

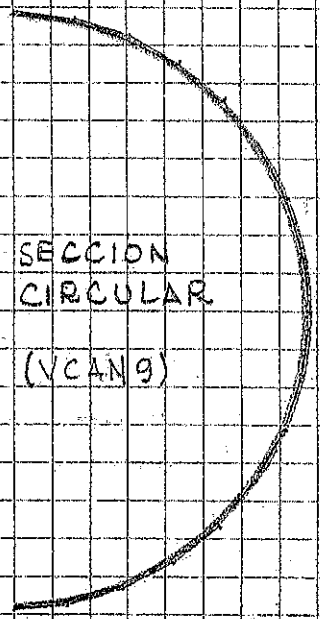

0 10 20 mt

ESCALA GRAFICA

MOMENTOS FLECTORES EN ESTADO DE CARGA CORRESPONDIENTE A UN INCREMENTO DE VOLUMEN ALREDEDOR DEL TUNEL.

3% Δ 0.5M

0.5% Δ 2.0M.

FIGURA 8

ESTUDIO SECCIÓN DE ENSAYO (1995)

- A PARTIR DE LAS CONCLUSIONES DEL PRIMER ESTUDIO:
  - DOS TRAMOS DE ENSAYO DE ≥50M EN TÚNELES IV Y V, SEPARANDO LOS ETES ≥15M DE LAS SECCIONES YA PERFORADAS

- OBJETO:
  - OBSERVAR EL COMPORTAMIENTO A CORTO Y MEDIO PLAZO DE UNA SECCIÓN PRÁCTICAMENTE CIRCULAR EN TOBAS CON NIVELES ARCILLOSOS EN SOLERA, HASTIALES Y CLAVE.

- SECCIONES DE ANÁLISIS
  - SECCIÓN COMPLETA (BÓVEDA 30CM)
  - SECCIÓN CON SOSTENIMIENTO DE GUNITA (7CM
  - SECCIÓN SIN CONTRABÓVEDA

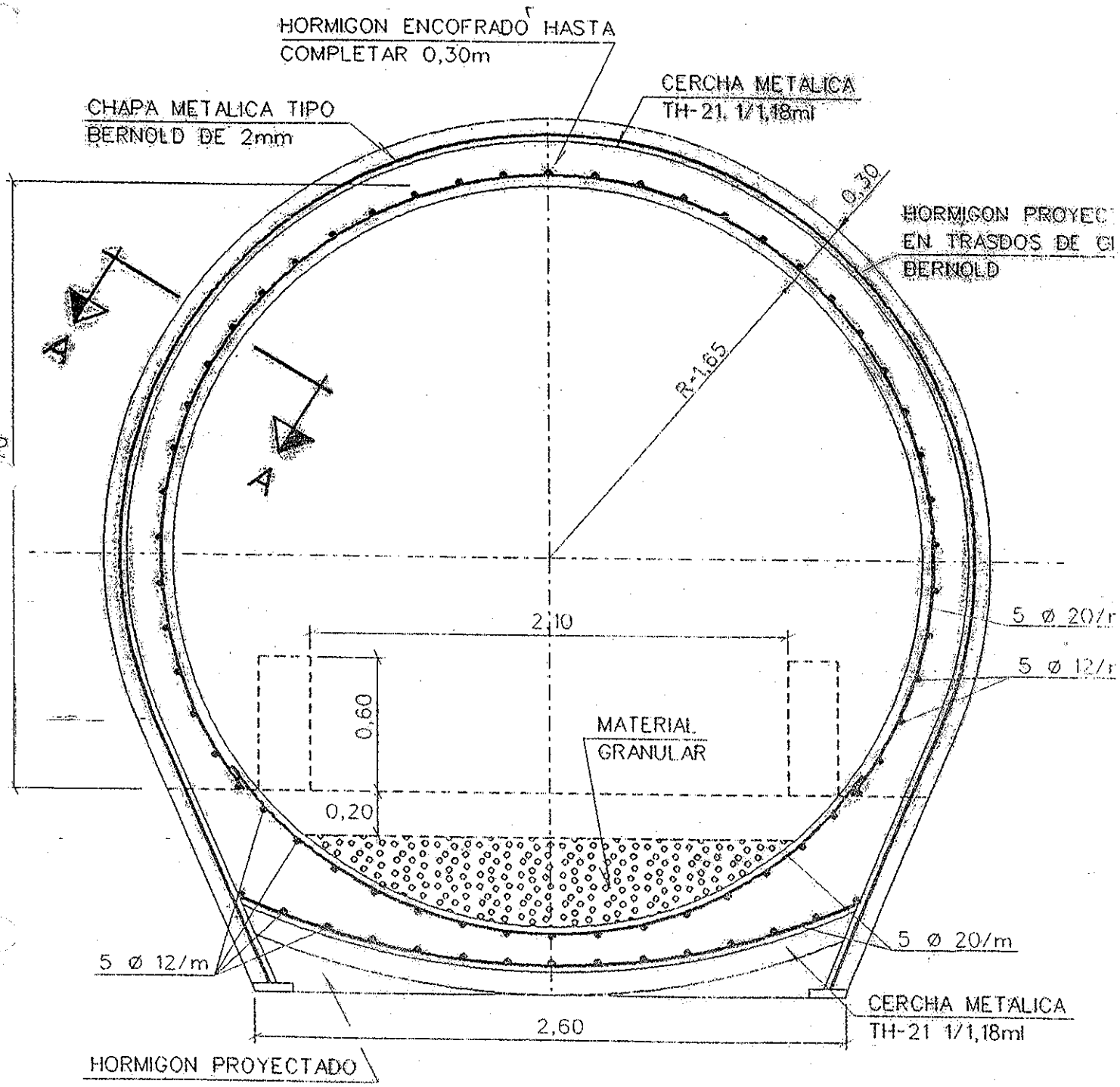

SECCION TIPO EN ARCILLAS

ESCALA-1/25

FIGURA 1

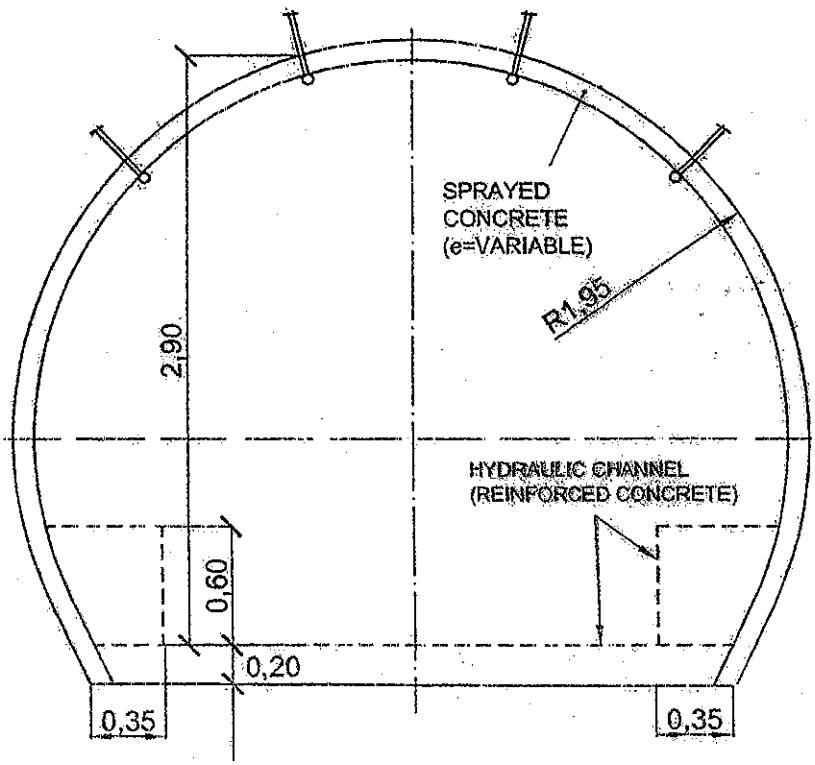

Fig. 12. Alternative cross-section (IV and V) considered for the experimental tunnel.

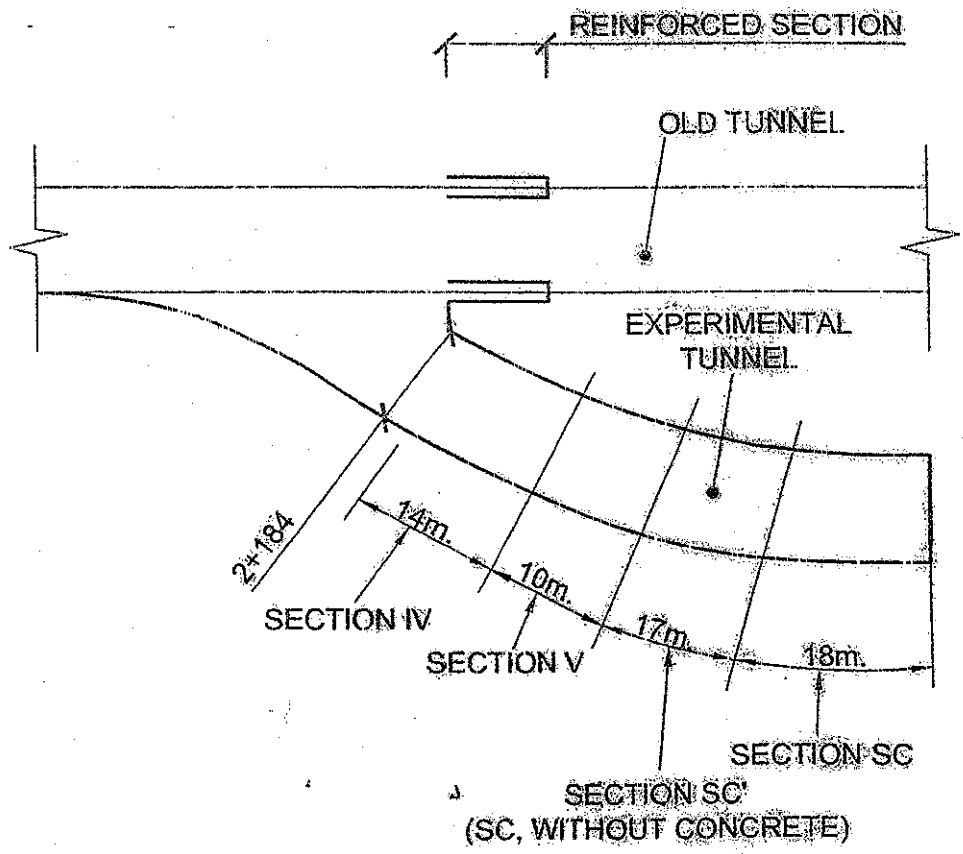

Fig. 13. Plan of the experimental gallery executed in tunnel V.

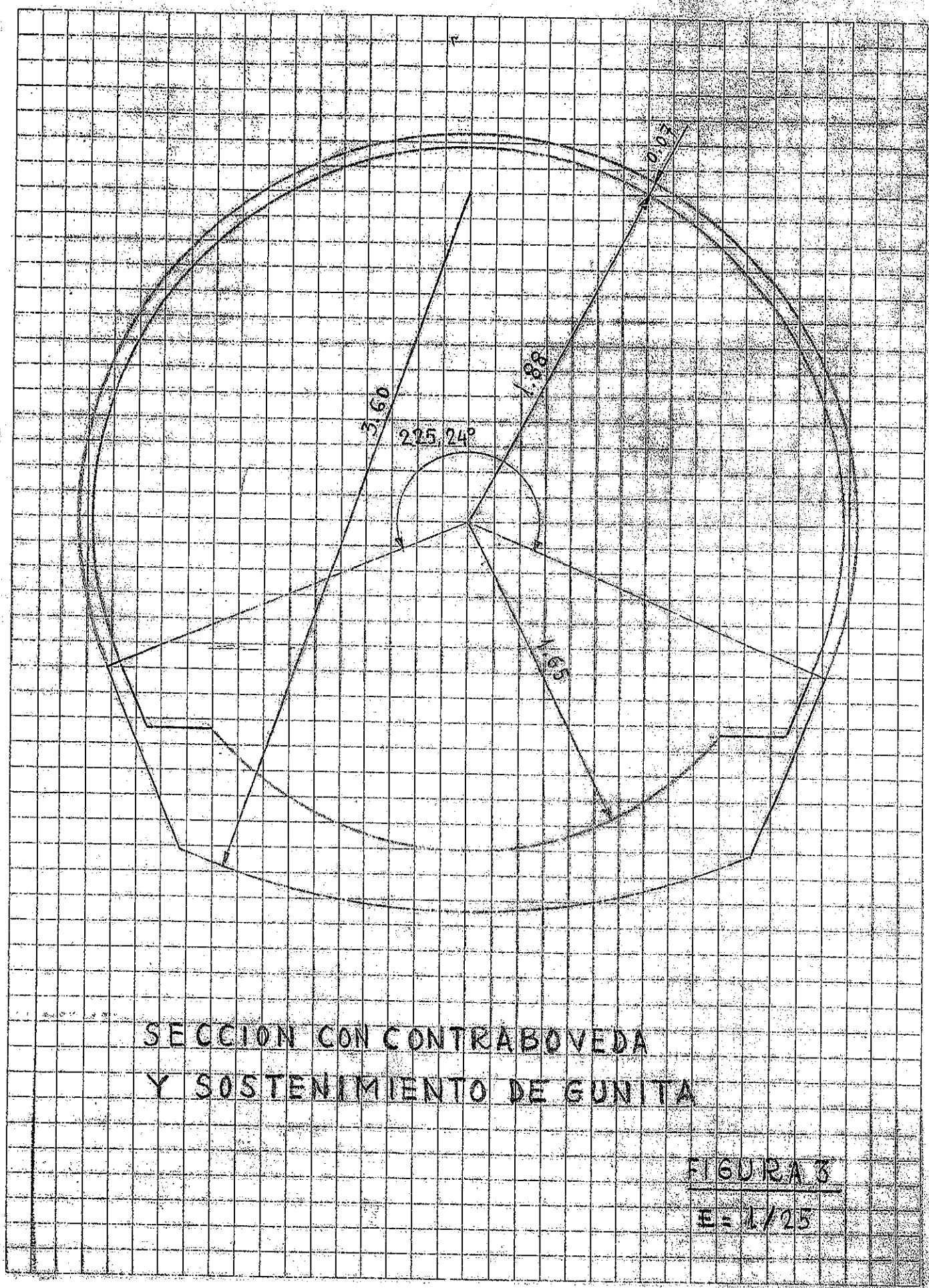

SECCION CON CONTRABOVEDA
Y SOSTENIMIENTO DE GUNITA

FIGURA 3

E = 1/25

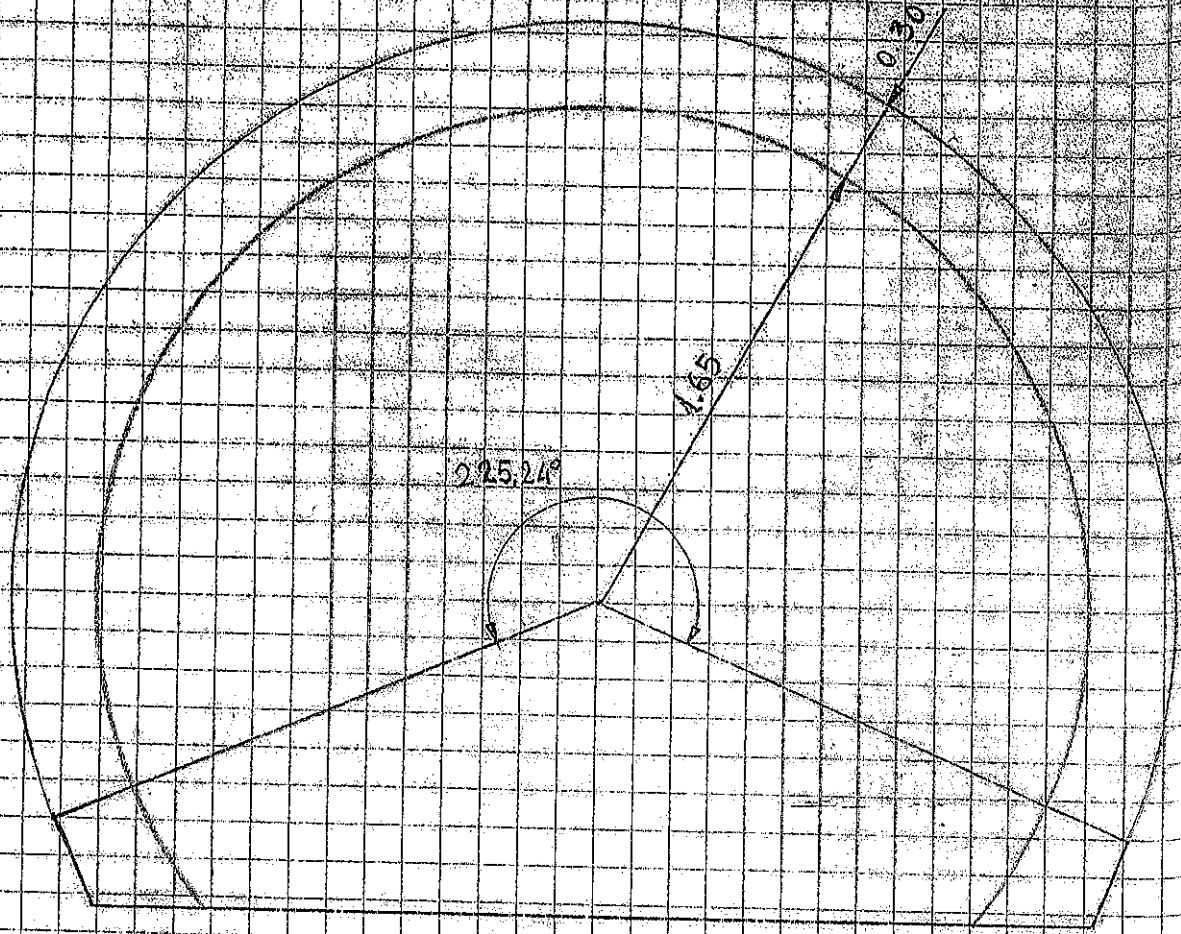

SECCION SIN CONTRABOVEDA

FIGURA 4

E= 1/25

MODELO DE CÁLCULO. ACCIONES

- MODELO EN 2D (DEFORMACIÓN PLANA)

- TERRENO: CUADRILÁTEROS DE OCHO NODOS
  TRIÁNGULOS DE SEIS NODOS
  (2 GDL/NODO)

  REVESTIMIENTO: ELEMENTO VIGA DE 2 NODOS
  (3 GDL/NODO)

- ESTADO DE CARGA:
  - AUMENTO DE VOLUMEN DE UNA CAPA HORIZONTAL DE ARCILLA SITUADA EN DISTINTAS POSICIONES.
  - VALOR MÁXIMO DEL AUMENTO DE VOLUMEN: 2%

- PARÁMETROS ELÁSTICOS:

  SUELO ARCILLOSO: $E = 600\ kp/cm^2$; $\nu = 0.2$.

  SUELO NO ARCILLOSO: $E = 15.000\ kp/cm^2$; $\nu = 0.25$

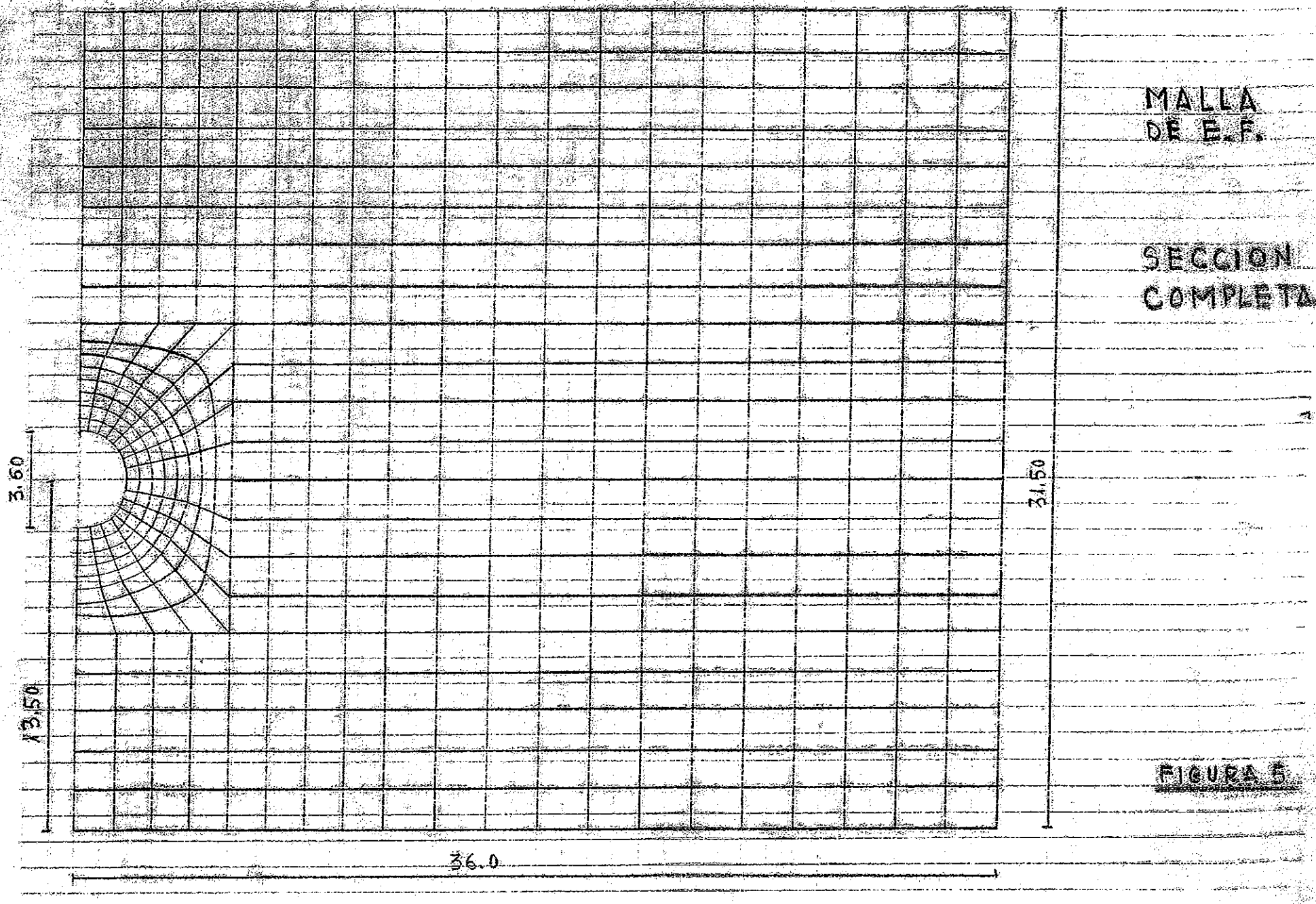

FIGURA 5.

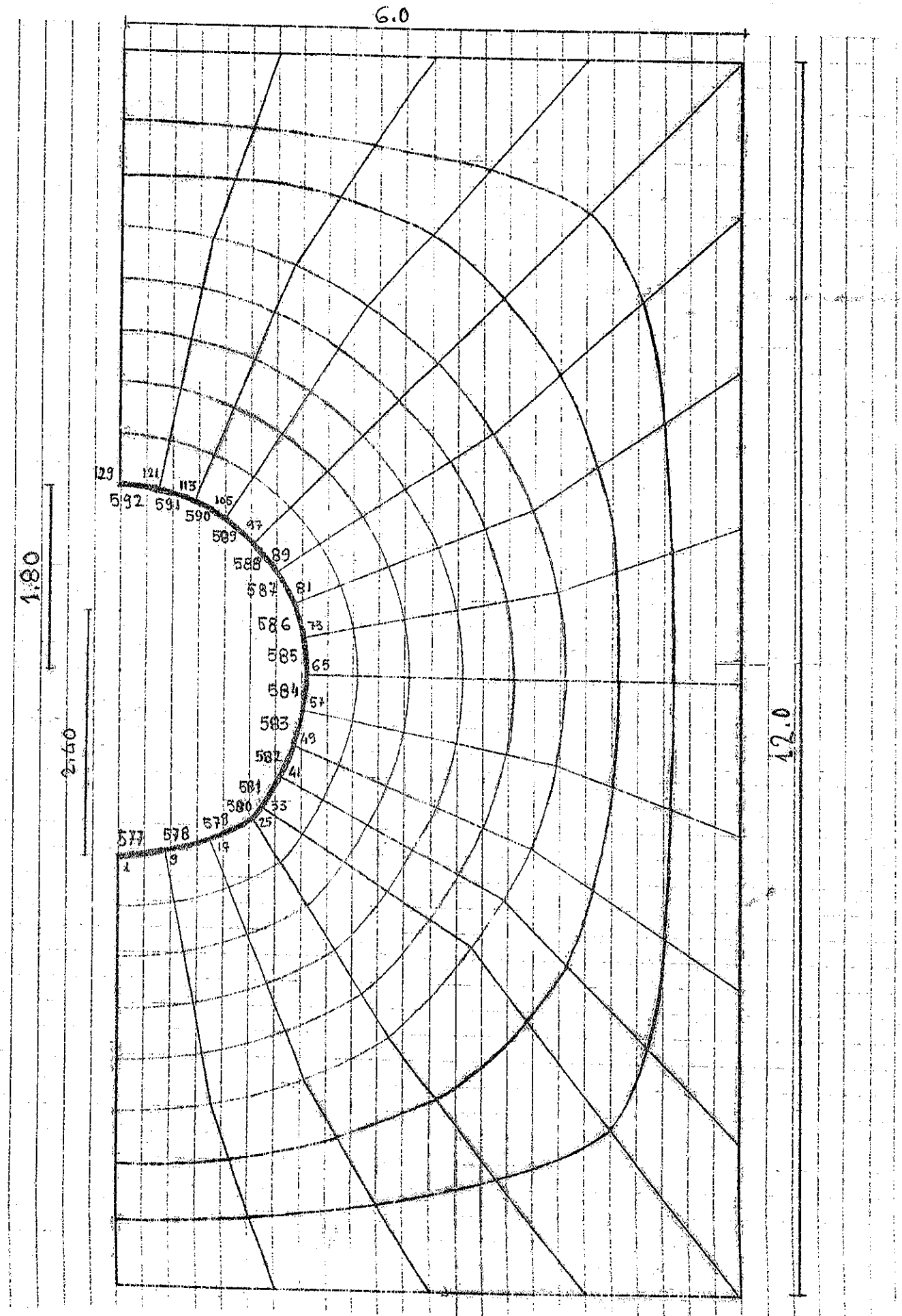

DETALLE DE LA MALLA DE E.F.
SECCION COMPLETA

FIGURA 5.A

ESFUERZOS Y MOVIMIENTOS

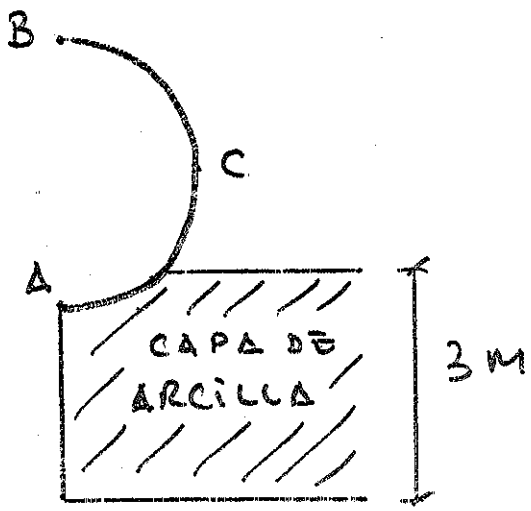

ATRASO (SECCIÓN COMPLETA)

$\sigma = (14.5 \pm 65.5)\ kp/cm^2$

$V_A = 2.5\ MM$; $V_B = 0.8\ MM$; $V_C = 0.6\ MM$

RETRASO (SECCIÓN CON SOSTENIMIENTO DE GUNITA)

$\sigma = (5 \pm 24)\ kp/cm^2$

$V_A = 1.0\ MM$; $V_B = 0.25\ MM$; $V_C = 0.2\ MM$

ESFUERZOS Y MOVIMIENTOS

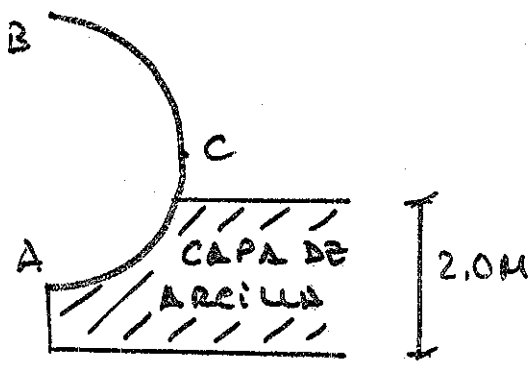

UTRAS 2 (SECCIÓN COMPLETA)

$\sigma = (9.5 \pm 37.5)\ kp/cm^2$

$V_A = 1.2\ MM$; $V_B = 1.0\ MM$; $U_C = 0.08\ mm.$

RTRAS 2 (SECCIÓN CON SOSTENIMIENTO DE GUNITA)

$\sigma = 16.5 \pm 38.5$

$V_A = 0.25\ MM$; $V_B = 0.3\ MM$; $U_C = 0.07\ MM.$

ESFUERZOS Y MOVIMIENTOS

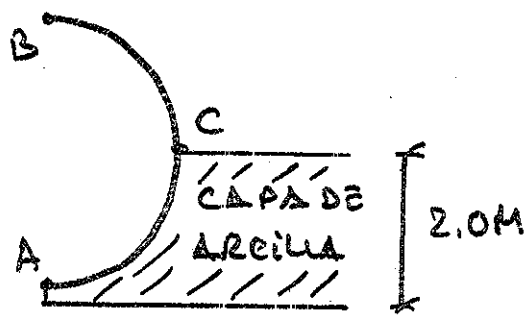

VTRAS 3 (SECCIÓN COMPLETA)

$\sigma = (-2.5 \pm 81)\ kp/cm^2$

$V_A = -0.3\ MM$; $V_B = 0.85\ MM$; $V_{cc} = -0.5\ MM$.

RTRAS 3 (SECCIÓN CON SOSTENIMIENTO DE GUNITA)

$\sigma = (2.5 \pm 60)\ kp/cm^2$

$V_A = -0.4\ MM$; $V_B = 0.3\ MM$; $V_{cc} = -0.1\ MM$

ESFUERZOS Y MOVIMIENTOS

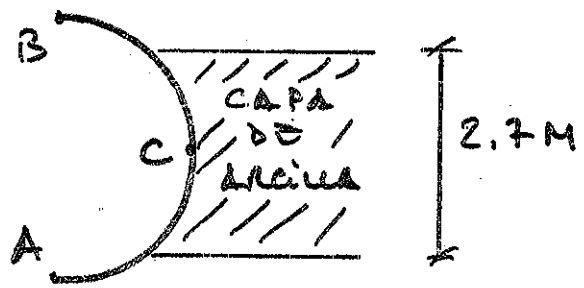

VTRAS4 (SECCIÓN COMPLETA)

$\sigma = (-3.5 \pm 97.5)\ kp/cm^2$

$V_A = -0.7\ MM$; $V_B = 1.0\ MM$; $V_C = -1.5\ MM$

RTRAS4 (SECCIÓN CON SOSTENIMIENTO DE GUNITA)

$\sigma = (18.5 \pm 86)\ kp/cm^2$

$V_A = -0.3\ MM$; $V_B = 0.5\ MM$; $V_C = -1.5\ MM$

ESTADOS
DE CARGA

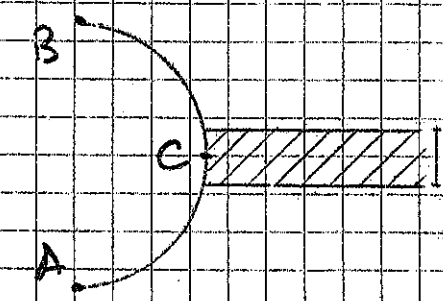

DTRAS 1 (SEC. COMPLETA)

$\sigma = (-10 \pm 26)\ kp/cm^2$

$V_A = -0.07\ mm \quad \| \quad V_C = -0.15\ mm$

$V_B = 0.16\ mm$

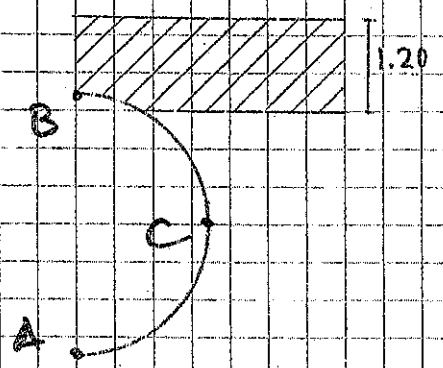

DTRAS 2 (SEC. COMPLETA)

$\sigma = (12 \pm 21)\ kp/cm^2$

$V_A = -0.3\ mm \quad \| \quad V_C = 0.3\ mm$

$V_B = -1.2\ mm$

SITUACION DE LA
CAPA DE ARCILLA

FIGURA 7

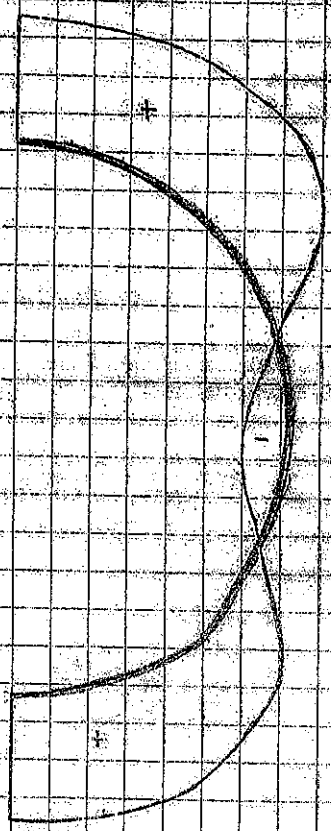

LEY DE ESFUERZOS AXILES

0 ——— 50 t

ESCALA GRAFICA

(-) TRACCION

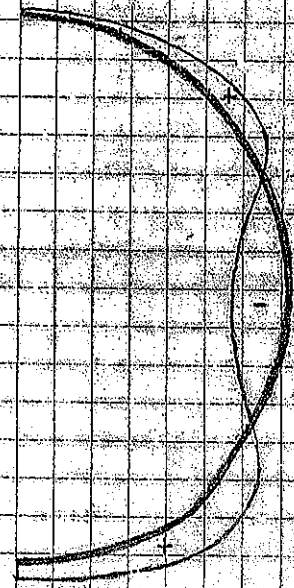

LEY DE MOMENTOS FLECTORES

0 ——— 30 mt

ESCALA GRAFICA

(-) +

ESFUERZOS EN EL ESTADO DE CARGA NTRAS 4
CAPA DE ARCILLA CENTRADA
CON EL EJE DEL TUNEL. POTENCIA: 2.7 M.

FIGURA 10

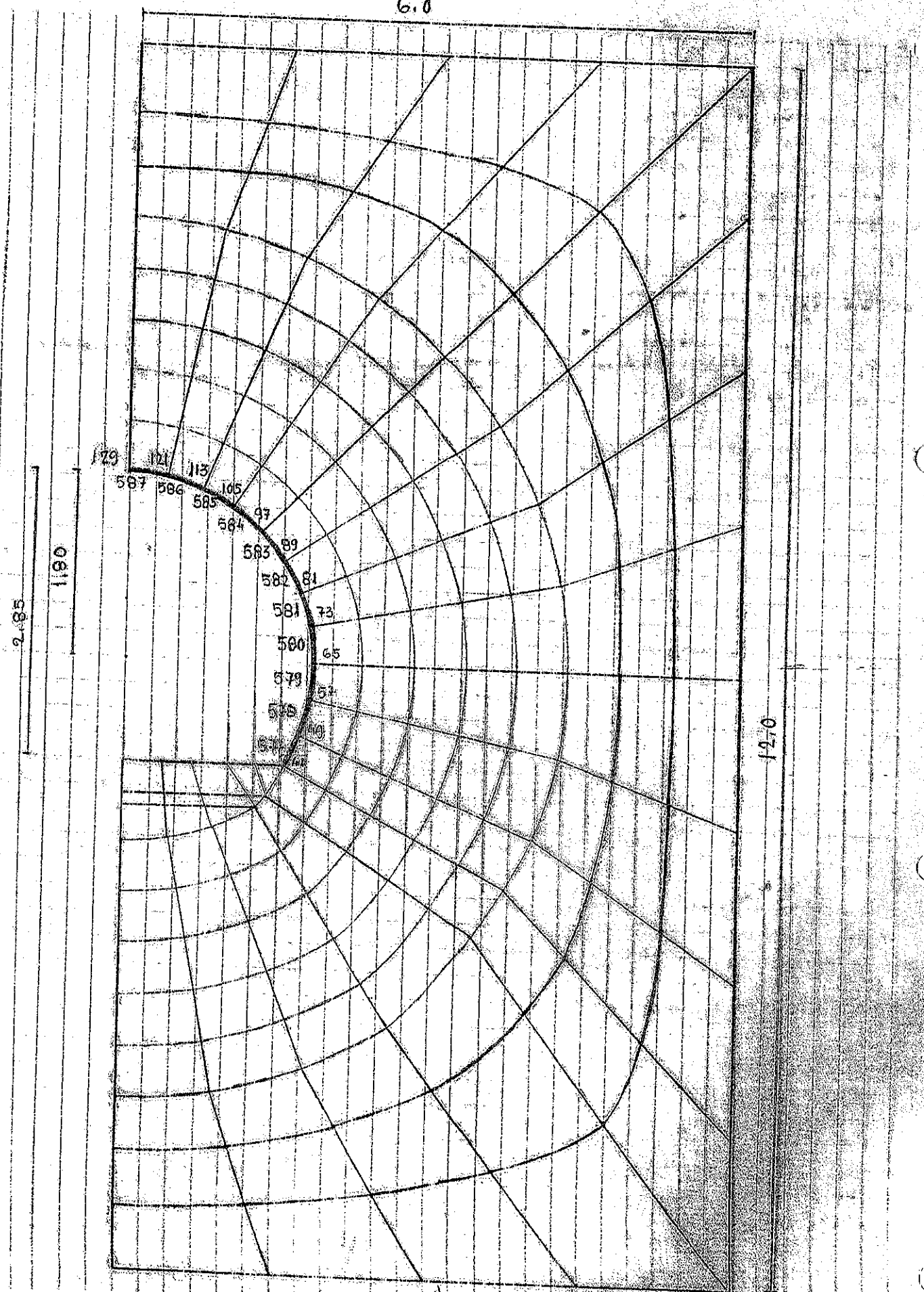

DETALLE DE LA MALLA DE E.T.
SECCION SIN CONTRABOVEDA

FIGURA 8.A

ESTADOS DE CARGA

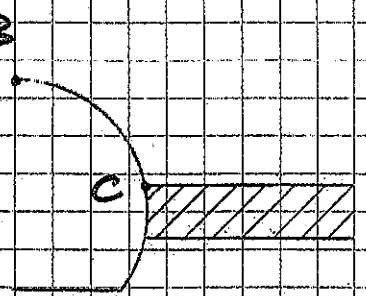

ATRAS 1 (SEC. SIN CONTRABOVEDA)

REVESTIMIENTO 30 CM.

$\sigma = (-9,5 \pm 26,5)$ Kp/cm²

VB = 0.17 mm

Uc = -0.15 mm.

REVESTIMIENTO 15 CM.

$\sigma = (-18 \pm 68)$ Kp/cm²

VB = 0.2 mm

Uc = -0.30 mm.

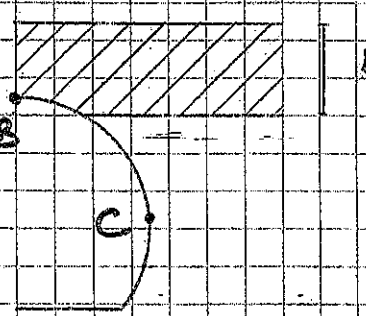

ATRAS 2 (SEC. SIN CONTRABOVEDA)

REVESTIMIENTO 30 CM

$\sigma = (12 \pm 20,5)$ Kp/cm²

VB = -1.2 mm

Uc = 0.3 mm

REVESTIMIENTO 15 CM

$\sigma = (25 \pm 35)$ Kp/cm²

VB = -1.4 mm

Uc = 0.34 mm.

SITUACION DE LA CAPA DE ARCILLA

FIGURA 9

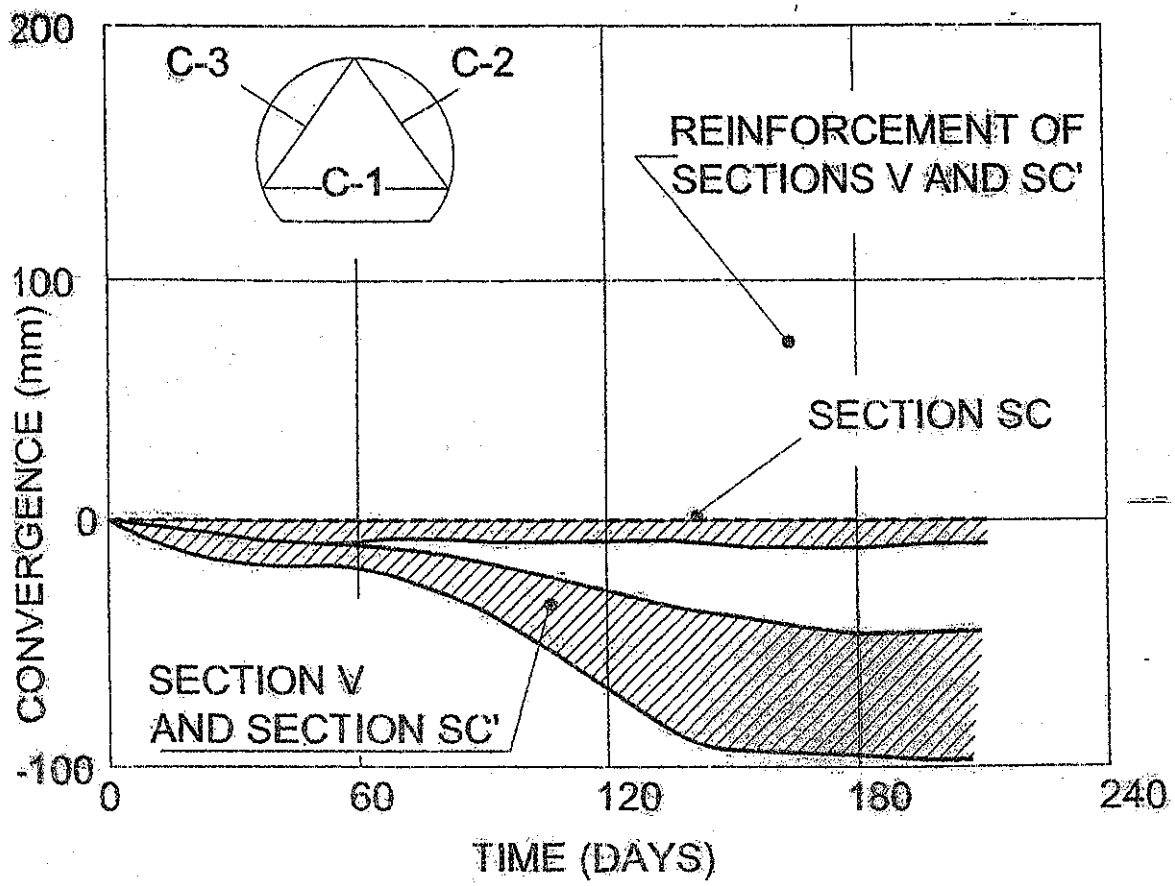

Fig. 14. Convergences measured in the experimental gallery

OPTIMIZACIÓN DE LA SECCIÓN

- EJECUTADO EL SOSTENIMIENTO Y LA CONTRABÓVEDA SE REGISTRARON CONVERGENCIAS ENTRE 0.6 MM Y 1 MM EN MÁS DE 40 SECCIONES Y ENTRE 3 Y 4 MM EN 4 SECCIONES

- MEDIANTE UN ANÁLISIS RETROSPECTIVO SE DETERMINÓ EL CAMBIO DE VOLUMEN:

CONVERGENCIA DE 4 MM:

1.13% Δ 0.5 M

0.28% Δ 2 M.

CONVERGENCIA DE 1 MM:

0.28% Δ 0.5 M.

0.07% Δ 2 M.

REVESTIMIENTO PROPUESTO.

REVESTIMIENTO TIPO A

HORMIGÓN PROYECTADO CON FIBRAS DE ACERO CON ESPESOR DE 15CM, EN SECCIONES DONDE EL NIVEL DE ARCILLA SE SITÚA EN CLAVE O EN CONTRABÓVEDA CON ESPESOR INFERIOR A 2.5 - 3.0 M.

REVESTIMIENTO TIPO B

HORMIGÓN PROYECTADO CON FIBRAS DE ACERO CON ESPESOR DE 20 CM, EN SECCIONES DONDE EL NIVEL DE ARCILLA SE SITÚA EN HASTIALES Y SE HAN MEDIDO CONVERGENCIAS INFERIORES A 1 MM.

REVESTIMIENTO TIPO C

HORMIGÓN PROYECTADO CON FIBRAS DE ACERO CON UN ESPESOR DE 20CM Y MALLA ELECTROSOLDADA (Ø6, 15x15), EN SECCIONES DONDE EL NIVEL DE ARCILLA SE SITÚA EN HASTIALES Y SE HAN MEDIDO CONVERGENCIAS DE 3-4 MM.

ELEMENTS

MAT NUM

AN

JUN 8 2006
17:08:12

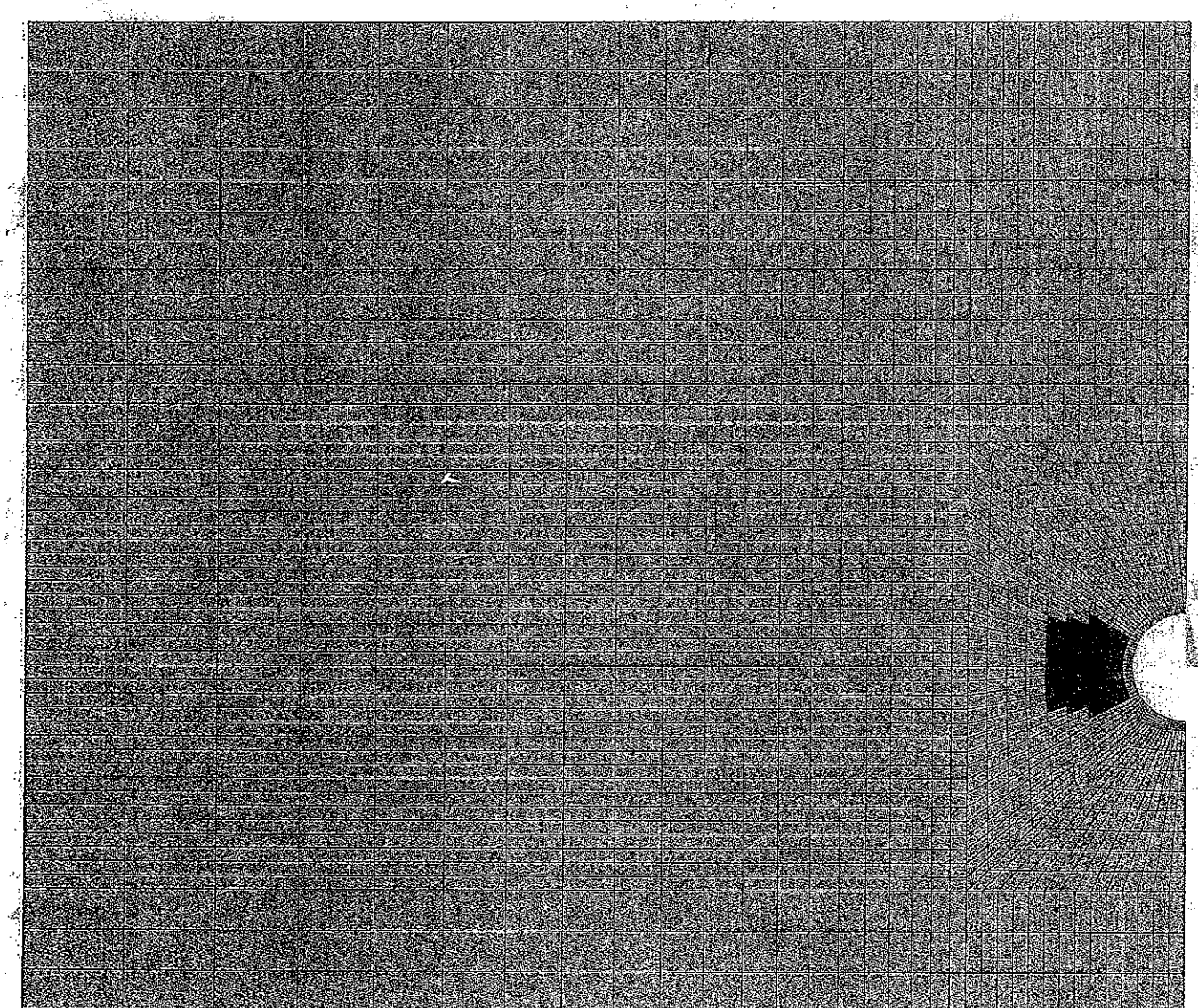

TRASVASIJR, TUNEL B

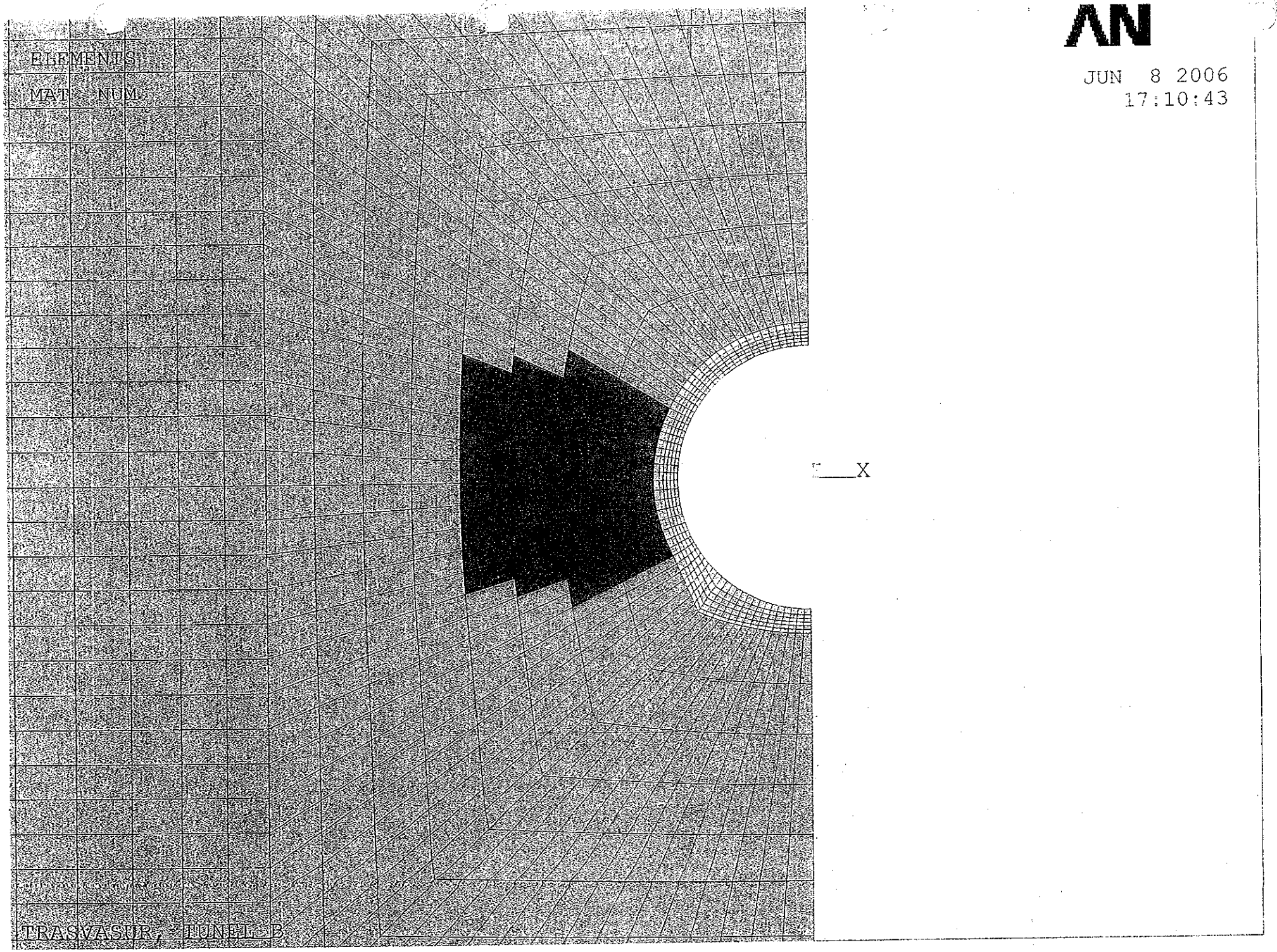
ELEMENTS
MAT NUM
AN
JUN 8 2006
17:10:43
X
TRASVASUR, TUNEL B

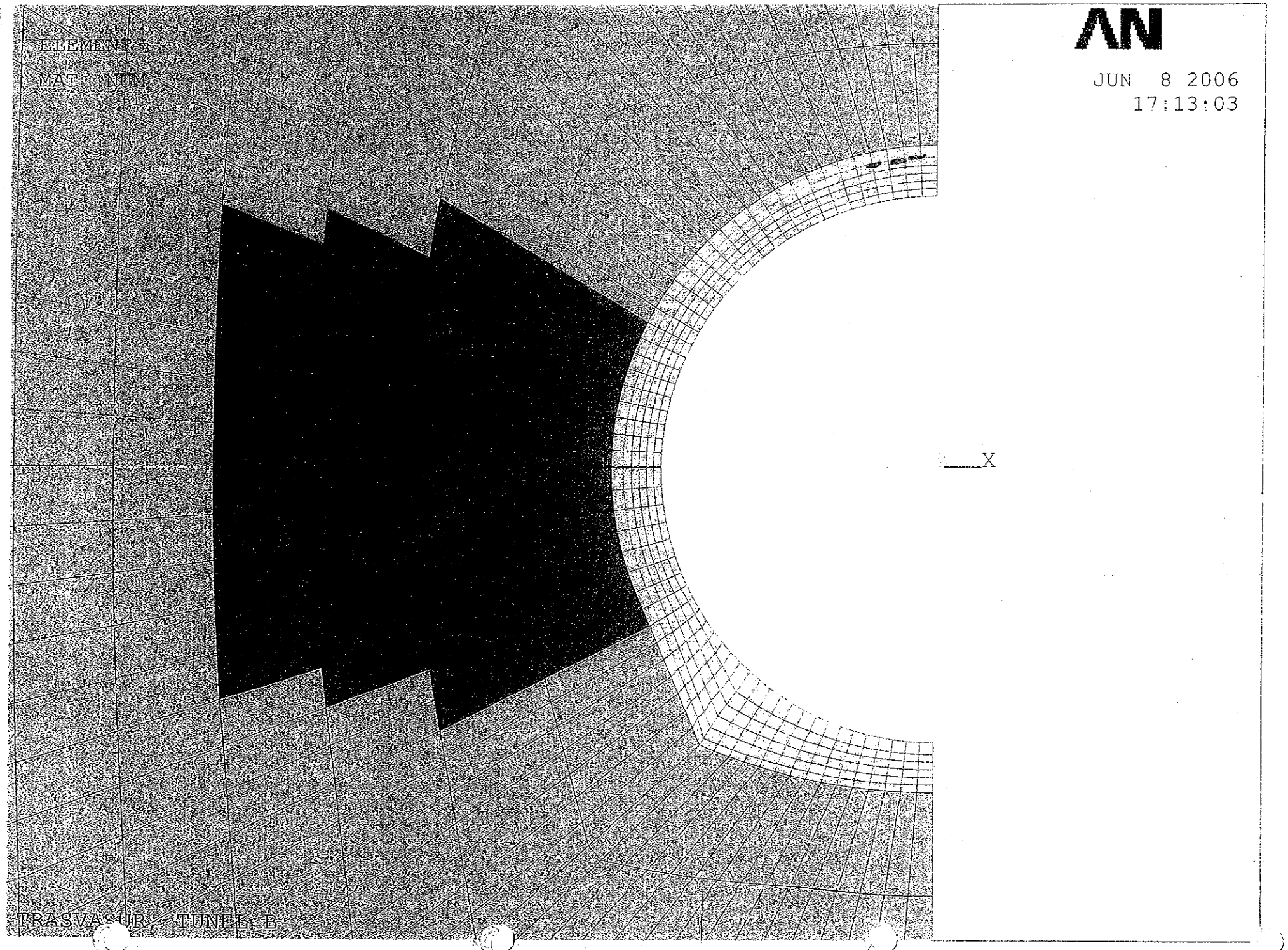
ELEMENTS
MAT NUM
AN
JUN 8 2006
17:13:03
X
TRASVASUR_TUNEL_B